

Review

Not peer-reviewed version

---

# Chiral Minerals

---

[David Avnir](#)\*

Posted Date: 7 August 2024

doi: 10.20944/preprints202408.0524.v1

Keywords: chirality; enantiomorphs; minerals; space-groups; formation; properties



Preprints.org is a free multidiscipline platform providing preprint service that is dedicated to making early versions of research outputs permanently available and citable. Preprints posted at Preprints.org appear in Web of Science, Crossref, Google Scholar, Scilit, Europe PMC.

Copyright: This is an open access article distributed under the Creative Commons Attribution License which permits unrestricted use, distribution, and reproduction in any medium, provided the original work is properly cited.

Review

# Chiral Minerals

David Avnir

Institute of Chemistry and Center for Nanoscience and Nanotechnology, the Hebrew University of Jerusalem, Jerusalem 9190401, Israel; david.avnir@mail.huji.ac.il

**Abstract:** Hundreds of minerals are chiral, that is, they appear in nature in two forms – left-handed and right-handed. Yet except for quartz, that key structural property remained, by-and-large in the shadow of the world of minerals in research, in museum displays, and for collectors. This review is devoted for providing a full picture of chiral minerals in nature. It starts with a general outline of the crystallographic background needed for the characterization of chiral minerals, continues with a detailed description of the many chemical and physical processes leading to their formation, follows with their chemical reactivities and transformations, with their physical properties, and with the ways to analyze and identify them. Many tables with listings of the various types of chiral minerals, are provided. It is hoped that this review will spark interest in this aspect nature's crystals.

**Keywords:** chirality; enantiomorphs; minerals; space-groups; formation; properties

---

## Contents

1. Introduction
2. Elements of crystallography of chiral minerals
  - 2.1 The relation between symmetry and chirality
    - 2.1.1 Enantiomorphism
    - 2.1.2 Symmetry elements, point-group symmetries, and their relation to chirality
  - 2.2 The lattice system
  - 2.3 The unit-cell (UC)
  - 2.4 The glide symmetry elements and the helical handedness labeling
  - 2.5 Space-group symmetry
    - 2.5.1 The space-group symmetry label of chiral crystals
    - 2.5.2 Chiral crystals - Söhncke space-group symmetries
  - 2.6 The asymmetric unit
  - 2.7 Conglomerates and racemates
3. The chiral minerals found in nature
  - 3.1 The abundance of chiral minerals and the “missing glove” situation
  - 3.2 Chiral minerals in the 22 enantiomorphic space-group symmetries
  - 3.3 Chiral minerals in the 43 non-enantiomorphic Söhncke space-groups
  - 3.4 Chiral organic and carbonate minerals
  - 3.5 Chiral polymorphic phase-transitioned minerals
4. Formation and transformations of chiral minerals
  - 4.1 Crystallization from the melt
  - 4.2 Chirality aspects of crystallization of minerals from aqueous solutions
  - 4.3 Polymerizations leading to chiral minerals
    - 4.3.1 The silicates
    - 4.3.2 Opals
    - 4.3.3 Ambers
  - 4.4 Chemical transformations of chiral minerals
    - 4.4.1 Hydrolyses
    - 4.4.2 Carbonations

- 4.4.3 Oxygenations
- 5. Chirality of the macroscopic mineral
  - 5.1 Molecular level descriptors of the macroscopic crystal
    - 5.1.1 The crystal class
    - 5.1.2 The crystal forms
  - 5.2 Chiral habits of minerals
    - 5.2.1 Growth conditions and randomness as sources of habit chirality
    - 5.2.2 Chiral twins
    - 5.2.3 Chiral habits of biominerals
  - 5.3 Chiral gemstone minerals
  - 5.4 Handedness labeling of the chiral minerals
    - 5.4.1 The problem of handedness labeling
    - 5.4.2 The enantiomeric excess
- 6. Physical, analytical and chemical properties of chiral minerals
  - 6.1 The diastereomeric interactions of chiral minerals with polarized light
  - 6.2 The interaction with x-rays and electrons: Absolute chiral configuration determination
  - 6.3 Physical properties of non-centrosymmetric crystals
  - 6.4 Surface chirality: the diastereomeric interactions of chiral minerals with chiral molecules
  - 6.5 Property/chirality correlations: Quantifying the degree of chirality

## 1. Introduction

While chirality of crystals – having left-handed and right-handed versions - has been intensively studied and reviewed (Flack, 2003; Thompson and Watkin, 2009; Rekis, 2020; Dryzun and Avnir, 2012), the literature of chirality as a key structural feature of the hundreds of minerals that have that property, has been limited, sporadic and vague, and, to the best of my knowledge, not comprehensively reviewed. Quartz, the most common chiral mineral is the only exception with voluminous literature discussing and describing its chirality in detail (The Quartz Page, <http://www.quartzpage.de/>; Götze et al, 2021), but, by and large, with some additional examples detailed below, it stops there. Chirality should be emphasized as a central structural feature of minerals because the left-handed and right-handed versions of chiral minerals are different from each other and different from achiral minerals, not only structurally but also in aspects of their physical, chemical and biochemical properties.

The vast majority of minerals are crystalline, and therefore crystallography, in particular chiral aspects of it, is a needed background for this review. One of the main aims of this review is to lead the non-crystallographer geologist and mineralogist into an overview of the main concepts needed for identifying and analyzing chiral minerals, while providing useful, straight forward instructions. That necessary background is the topic of Section 2, and to ease the reading of this part, the needed terms are in ***bold italics*** when appearing and defined for the first time. Readers of this part for which that Section is the first encounter with the elements of crystallography are encouraged to follow the cited educational references for graphics (which are referred to with hyperlinks, to be opened while reading). There are several excellent educational sources, such as Hoffmann's textbook (Hoffmann, 2016) and its accompanying series of lectures at (Frank Hoffmann, <https://www.youtube.com/@FrankHoffmann1000>).

Section 3 is then devoted to a display of the broad picture of the chiral minerals in nature and to their various classifications. Attention is drawn in that Section to the “missing-glove” situation: Despite the fact that chiral minerals must appear in nature in two distinctly different forms – the left-handed and right-handed forms (gloves) – the number of chiral minerals for which these two forms are explicitly isolated, characterized or displayed in publications or in mineral collections is extremely limited. Section 4 is devoted to the rich family of chemical processes and physical processes which form chiral minerals, including phase-transitions, crystallizations, polymerizations and chemical transformations. While the first three main Sections 2-4 focus on the molecular-level aspects of chiral minerals, in Section 5 we move to the chirality of the macroscopic mineral, namely to their chiral

shapes, forms and habits including gemstones and biominerals. Finally, Section 6 summarizes the physical, analytical and chemical properties of chiral minerals, including optical rotation, x-ray diffractions, adsorption on chiral minerals, methods of distinguishing between the left- and right-handed forms, ending the review with the concept of quantifying the degree of chirality of a chiral mineral.

## 2. Elements of Crystallography of Chiral Minerals

### 2.1. The Relation between Symmetry and Chirality

The main structural characteristic of crystals is their symmetry on the molecular and sometimes on the macroscopic scales, and identifying chirality of a crystal requires knowledge of these symmetry features. This is so, because symmetry and chirality are structural properties which are intimately linked. The grounds for this relation are explained now:

#### 2.1.1. Enantiomorphism

Chirality can be defined in several ways, and here is an elementary one: *An object is chiral if it has left-handed and right-handed forms* (either both real, or one real and the other virtual). These two related forms are generally termed **enantiomorphs** (enantiomorphic crystals, for instance). In the specific case of molecules and at the molecular level in general, this pair of forms is termed **enantiomers** (for instance, right- and left-handed amino acids). The main identifying property of a pair of enantiomorphs (or enantiomers) is that they are mirror images of each other, which cannot coincide with each other by their superposition (such as a pair of gloves). This non-superimposability is a simple test for detection of chirality, and it serves also as a more common definition of chirality: *An object is chiral, if it cannot be superimposed with its mirror image*. Thus, enantiomorphs are very similar and very different at the same time: They are similar because they are mirror reflections of each other; and they are different, because they cannot be superimposed. From the point of view of symmetry, the simplest manifestation of the non-superimposability of enantiomorphs is that the chiral object must not have mirror symmetry. This is so, because the reflection of a mirror-symmetric object coincides with the original and therefore both can be fully superimposed, leading to **achirality**. In fact, not only mirror symmetry renders an object achiral, but other symmetries do so as well. In this section we generalize the non-superimposability rule to include these other symmetries, and also see which symmetries chiral objects may have.

#### 2.1.2. Symmetry Elements, Point-Group Symmetries, and Their Relation to Chirality

**Symmetry**, in its general geometrical definition, is the property of an object of being invariant to transformations, including translation, reflection, rotation and change of scale, or to combinations of these. A **symmetry operation** is a movement of an object into a new orientation in such a way that resulting moved object is indistinguishable from the original object. The movement may be either real - such as rotation - termed **proper symmetry**, or imaginary - such as reflection through a mirror - termed **improper symmetry**. The symmetry operation movement is carried out with a **symmetry element** - with a line which is a rotation axis, with a plane which is reflection mirror, or with a point (in case of inversion symmetry - see below). Let us now detail the properties of the various symmetry operations and their relation to chirality:

\* In **rotational symmetry** the symmetry element is an axis of rotation which passes through the center point of an object. The rotational symmetry operation brings the object symmetrically to a shape-identical self (for graphics of this and the other symmetry elements, see (Symmetry@Otterbein, <https://symotter.org/tutorial/intro>). Rotational symmetry is defined by the fraction of a full rotation,  $360^\circ/n$ , which brings the object to its original shape. The integer  $n$  is the **order** of the rotation. For instance, for the rotational symmetric recycling symbol



the relevant symmetry rotational steps are of  $120^\circ$  around a perpendicularly centered axis of rotation, that is  $n = 3$ , completing a full rotation after 3 such steps ( $120^\circ$ ,  $240^\circ$ ,  $360^\circ$ ); each of these three steps is a symmetry operation.

The labeling of symmetry elements is done (unfortunately) mainly by two methods: The *Schoenflies (Sch)* notation convention, and the *Hermann-Maguin (HM)* notation convention. These are commonly used in crystallography, and appear in most mineral listings. To avoid confusion, *Sch* notation will appear in *italics*, and HM in regular fonts. The rotational symmetry, it is denoted in the HM notation by the order number,  $n$ , or in the *Sch* notation by  $C_n$ . For instance, the recycling symbol has a 3 or  $C_3$  threefold rotational symmetry, and the three symmetry operation steps are labeled with superscript,  $C_3^1$ ,  $C_3^2$  and  $C_3^3$ , for  $120^\circ$ ,  $240^\circ$  and  $360^\circ$ , respectively. A symmetric object, the symmetry of which is characterized only by rotational elements, is chiral, such as in a three-blades propeller of rotational 3 symmetry, for which a pair of enantiomorphs exists:



Thus, objects which are rotationally symmetric and only of these symmetries, are chiral.

For what follows it is important to note the symbol of rotational symmetry do not provide information about the enantiomorphism of that chiral object, namely whether it is left-handed or right-handed; this will require additional labeling, to which we return later on.

\* Closely related to the rotational symmetry is the case where the object has no symmetry at all (*asymmetric*). This is so because a full  $360^\circ$  rotation, brings the object back to itself. This is the *identity* symmetry operation, and using the rotational symmetry terminology, such objects are denoted by the number 1 in HM or  $C_1$  (or  $E$ ) in *Sch*. *Objects which do not have any symmetry are chiral* (because their reflection is not superimposable with the original).

\* *Mirror symmetry* is characterized by exact and full (virtual) superposition of an object with its mirror image. To be a mirror-symmetric object requires that the object be of *bilateral symmetry*, that is, that it has at least one symmetry plane that bisects it into identical or mirror-symmetric halves. The symmetry element – the bisecting mirror plane – is denoted  $m$  in HM or  $C_s$  (also  $\sigma$ ) in *Sch*. Objects with this symmetry (with or without additional rotational symmetries) are not chiral (achiral), because, as just mentioned, such objects superimpose with their mirror image. Most minerals have this and/or the next two symmetry elements, *and are therefore achiral*.

\* The combination of reflection and rotation, *roto-reflection*, is denoted in HM with an even number numeral and with an upper bar (macron),  $\bar{n}$  (also with a minus sign,  $-n$ ), or  $S_n$  in *Sch*. For instance,  $\bar{4}$  or  $-4$  or  $S_4$  denotes a fourfold rotation axis+reflection through a mirror perpendicular to it (Symmetry@Otterbein, <https://symotter.org/tutorial/intro>). Since this combination contains reflection, *objects with this symmetry are achiral*.

\* A special case of roto-reflection which has its own label (because it is very common) is the center point which is the element for *inversion symmetry* operation. It is a roto-reflection combined of a rotation of order 2 ( $180^\circ$ ) and reflection, and is denoted  $\bar{1}$  (also  $-1$ ), or  $C_i$  (also  $S_2$  or  $i$ ). Since this symmetry is part of the roto-reflection family, *minerals with inversion symmetry are achiral*.

Symmetric objects may be characterized by more than one symmetry element, and the group of symmetry elements which describe such objects, is termed *point-group symmetry* ("point" because all of the symmetry elements gathered in that group pass through at least the same single point, which is left in place when the symmetry is operated). *Point group symmetries which describe chiral objects contain only rotational elements and the identity*. For instance, the point group which is marked  $D_4$ , is composed of one  $C_4$ , three  $C_2$  and the identity  $C_1$  rotational axes. On the other hand, the point group which describes the symmetry of an octahedron,  $O_h$ , (which we mention in the next Section), contains 24 planes of symmetry (as well as 24 rotational symmetry elements, and therefore describes achiral objects. Group-theory tells us which specific symmetry elements of those listed above can be gathered into point-groups, and there are infinite such combinations. However, crystals, because of their 3D symmetric space-filling restrictions, are quite limited in the allowed symmetry point groups – only 32 – and these are detailed in the next section and in Section 5.1.1 (The crystal class).



## 2.2. The Lattice System

Crystals are highly ordered repeated arrays with 3D translational symmetry, of building blocks, which may be atoms (such as in metallic crystals), ions (ionic crystals), molecules (molecular crystals), polymers or their segments (covalent crystals), or any combination of these. The shapes and symmetries of these ordered arrays of molecular building blocks – the crystals – are described and classified in several ways.

The most elementary classification of a crystal is according to its *lattice* - an abstract mathematical entity defined its axial vector systems - within which one places the atoms of the crystal. One can visualize the lattice as composed of boxes, stacked in an ordered way (such as with ship containers), into which in each box one fills-in a repeating collection of atoms. The shapes of the parallelepipeds (boxes) which can be used for the periodic space filling are defined by the lengths and direction-angles of the three edges of that parallelepiped (vectors), emanating from one of its corners (the origin). For instance, if all three edges are of equal lengths and all angles are of 90°, the lattice is *cubic*, that is, the shape of the parallelepiped is of a perfect cube and so is the shape of the whole lattice, if tiled equally in all three dimensions. The elementary cube which builds the lattice is the most symmetric one – achiral octahedral point-group symmetry,  $O_h$ , and so is the lattice which is built into a larger cube with these Lego blocks. The least symmetric lattice is the *triclinic* for which all of the three edges and all three angles of the parallelepiped are different from each other; the point-group symmetry here is the achiral inversion symmetry,  $C_i$  (for graphics of the various lattices, see: (Chemicool Dictionary, [https://www.chemicool.com/definition/lattice\\_crystal.html](https://www.chemicool.com/definition/lattice_crystal.html)). The other crystal lattices are built from various intermediate combinations of lengths ratios and angles, and these are (along with their point-group symmetries) the *monoclinic* ( $C_{2h}$ ), *orthorhombic* ( $D_{2h}$ ), *tetragonal* ( $D_{4h}$ ), *hexagonal* ( $D_{6h}$ ), and the *rhombohedral* ( $D_{3d}$ ) lattices – a total of 7 lattices. Each of these is termed a *lattice system*.

These lattices are termed lattice systems (and not simply lattices), because they can give rise to several possible *lattice types* (or lattice varieties) by adding specific points to the points which occupy the corners of the parallelepiped (the *basis*). All-and all, when this is done, the number of crystallographic lattices – systems and their types - is 14, collectively known as *Bravais lattices* (Cristalografia, [https://www.xtal.iqf.csic.es/Cristalografia/parte\\_03\\_4-en.html](https://www.xtal.iqf.csic.es/Cristalografia/parte_03_4-en.html)). The most elementary lattice type is the *primitive* lattice-type, denoted **P**, representing only the points which occupy the corners of the parallelepiped. Then, if one adds lattice points at centered positions of the parallelepiped, the *body centered cubic* lattice, denoted **I**, is obtained. The *face centered cubic* lattice, denoted **F**, indicates additional face-centered points on all faces. The *single-face centered* lattice has an additional point at the center of one of the box's faces, denoted **S** (or **A**, **B**, or **C**, depending on which face has that point). There is also a notation for the rhombohedral presentation of the trigonal lattice, denoted **R**. The point-group symmetry of all lattice types which belong to a given lattice system, remain unchanged. For instance, the cubic lattice system has three lattice types - **P**, **I** and **F** – all of which are of octahedral symmetry,  $O_h$ .

None of the lattice systems is chiral – all are of achiral symmetry point groups. But if so, how can they represent chiral crystals? This is explained next:

## 2.3. The Unit-Cell (UC)

Having lattices all of which are achiral, where does the chirality of the crystal enter? It enters in the spatial arrangement of the atoms and molecules which are placed within one of the 14 Bravais lattices. Placing chiral building blocks in an achiral lattice does not erase the chiral properties of the chiral crystal. This is so because the *chirality is dictated by the molecular content* of the parallelepipeds that form the lattice, and not by the way these molecular building blocks are translationally packaged into the macroscopic crystal. It is indeed therefore that the classification of crystals symmetry is not only by their lattices, but by the combination of the lattice and molecular content symmetries – this leads to the space-group symmetry crystal-system classification, described in Section 2.5.

There are various options as to how to place the atoms relative to the lattice grid, that is, how to select the sub-set of atoms (molecular fragments, whole molecules, monomeric unit of a polymer, etc.) to represent the repeating unit of the crystal. The standard method is guided mainly by two instructions: Taking the minimal number of atoms needed for the repetitive space-filling tiling of the crystal; and placing them inside the box with at least partial coincidence – if possible - with the Bravais lattice points. This minimized atomic arrangement within the box is the **unit cell (UC)** of the crystal. The atoms may be at the corners, on the edges, on the faces coinciding with the lattice points or not, or be contained inside the box, that is, with any of the lattice types described in the previous Section

Note 1.

A distinction is made between three options of chiral molecular arrangements within the UC of the crystal: These are inherent chirality, conformational chirality and positional chirality. **Inherent chirality** refers to a molecular structure which retains its chirality, regardless of the conformation which it is capable to assume. The most common example is a carbon atom with 4 different substituents, which is also the main source of the chirality of biomolecules and of the few minerals that are derived from them. Since the biochemistry of planet Earth operates mainly (but not exclusively (Avnir, 2021)) on only one of the two enantiomers (**homochirality**; for instance, mainly “left-handed” L-amino acids and mainly “right-handed” D-sugars), the (rare) minerals based on inherently chiral biomolecules and their UCs, appear - unlike the conformationally or positional chiral minerals - as a single enantiomorphs. An example is fichtelite,  $C_{19}H_{34}$  (18-norabietane), described in more detail below. **Conformational chirality**, on the other hand, refers to chirality which is induced by a distortive intra-molecular motion which is frozen in the crystal (rotation, stretching, varying the bond-angle). For instance, the  $Si_3O_6$  molecular content of the UC of quartz, is an oxygen-linked  $SiO_4$  chain which assumes a helical conformation, thus leading to left- and right-handed enantiomorphs of the mineral. Furthermore, the  $SiO_4$  unit itself is slightly distorted from ideal tetrahedrality ( $T_d$ ) into chiral rotational  $C_2$ -symmetric conformer (Yogev-Einot and Avnir, 2003). Tetrahedral distortion into a chiral conformer in crystals is found in also in other  $AB_4$  species, such as in phosphates,  $PO_4^{3-}$  (Yogev-Einot and Avnir, 2007). In general, conformational chirality offers a much richer library of chiral species, because it is open to molecules or fragments which in their free forms are either achiral or chiral, and because molecules and their fragments have “endless” conformational options which can be frozen in a crystal. Conformational chirality is very common in minerals. Finally, there is the option of **positional chirality**: Here, two or more molecules – achiral, chiral, or an enantiomeric pair - pack into the UC in a mutual orientational arrangement which is chiral.

#### 2.4. The Glide Symmetry Elements and the Helical Handedness Labeling

The point-group symmetry elements described in section 2.1 suffice for the description of the macroscopic symmetry of the crystal (Section 5) and for the description of many – but not all – of the symmetries of the molecular building blocks of the crystal. However, for a full description of the molecular level symmetry, two additional elements are defined, which involve the crystal translational symmetry (and therefore are not included in the point-group symmetries which require a fixed point) – these are the **glide-plane** and the **roto-glide** (screw axis) symmetry elements (Hoffmann, <https://www.youtube.com/@FrankHoffmann1000>) which relate to the translational symmetry properties within the unit-cell (UC). Most of this section is devoted for the roto-glide, which is a key symmetry element of chiral crystals; and we then briefly describe the glide plane, which characterizes achiral crystals only.

The **roto-glide** (or **screw axis**) symmetry element combines helical operation with translational glide in the direction of the long axis of the helix, contained inside the UC. It describes chiral crystals because the helix is chiral, the enantiomorphs/enantiomers of which are the left or right-handed versions of the helix. The roto-glide element is denoted (in practice, mainly by the HM notation system) as  $n_m$  (also appears as  $nm$ ), where  $n$  describes the rotational symmetry component of the helix, that is, the rotational symmetry of the 2D-projection perpendicular to the helicity axis,  $z$ . The subscript  $m$  denotes the number of  $360^\circ/n$  rotational steps taken along the helix, namely, the gliding distance inside the UC, which brings the object to an undistinguishable same (the symmetry

operation) (Hoffmann, <https://www.youtube.com/@FrankHoffmann1000>). For instance, in the  $3_1$  (also appears as  $3_1$ ) notation, 3 is the rotation symmetry of the helix 2D projection, and the subscript 1 tell us that that the helical rotation of  $360^\circ/3=120^\circ$ , is followed by a  $1/3$ -UC glide along the long direction of the helix. Theory of crystallography tells us that only a limited set of rotational symmetries and their combinations can fulfil the space-filling restrictive condition of the lattices. These are the identity (1), the two-fold (2), three-fold (3), four-fold (4) and six-fold (6) rotational symmetries, and the associated helical roto-glides of  $2_1$ ,  $3_1$ ,  $3_2$ ,  $4_1$ ,  $4_2$ ,  $4_3$ ,  $6_1$ ,  $6_2$ ,  $6_3$ ,  $6_4$ , and  $6_5$ .

Out of these 11 roto-glide elements, 8 represent 4 enantiomorphic pairs:  $3_1$  and  $3_2$ ,  $4_1$  and  $4_3$ ,  $6_1$  and  $6_5$ , and  $6_2$  and  $6_4$ . The agreed convention is that the smaller m in each pair represents a right-handed roto-glide helix (the regular clockwise motion for penetrating a screw), for instance  $3_1$ , while the larger m - ( $3_2$ ) - represents the left-handed (counter-clockwise, unscrewing) roto-glide helix <sup>Note 2</sup>.

The 8 enantiomorphic roto-glide pairs  $3_1$ ,  $3_2$ ,  $4_1$ ,  $4_3$ ,  $6_1$ ,  $6_2$ ,  $6_4$ , and  $6_5$ , *always indicate a chiral crystal* and do not appear in achiral crystals. However,  $2_1$ ,  $4_2$ , and  $6_3$ , do not have enantiomorphs because each of them means a rotation of  $180^\circ$  with a  $1/2$ -UC glide, and that point is reached regardless of whether the rotation is to the left or to the right. Since these three elements are still rotation elements but they do not carry enantiomorphic information, they may describe both chiral (in conjunction with other rotational symmetries) or achiral crystals (in conjunction with other symmetry elements which are not rotations).

The second translational symmetry element is the *glide-plane* element, which represents the combination of a glide (translation) with a reflection. Its HM notation uses a lower-case letter (a...e or n) depending on the glide direction. Most translational glides are  $1/2$  of the UC, and some are also  $1/4$  of the UC. Crystals with this symmetry element are achiral, because they contain the reflection operation.

From the point of view of the chirality criterion, both the point group symmetry elements and the glide translational symmetry elements are put under a unified umbrella, divided into two types: Proper symmetry elements – which are the rotational, roto-glides and identity symmetries; and the improper symmetry elements – which contain mirror symmetry and its derivatives (roto-reflection, glide-plane). The chirality criterion is therefore:

*An assembly of atoms is chiral if its structure is characterized by rotational (proper) symmetry elements only*

Having that generalization for point groups and the glides, we can now move to the main identifier of a chiral crystal – its space group symmetry:

## 2.5. Space-Group Symmetry

### 2.5.1. The Space-Group Symmetry Label of Chiral Crystals

The main identifier of the molecular level symmetry/chirality of a crystalline mineral in all major mineral listings is its *space-group symmetry* (SGS, or “space-group”, in short)). The SGS combines into a single label the lattice-variety upper-case letter symbol (Section 2.2), and the symmetry elements within the UC including the glide-symmetries. The restriction imposed by the fact that the packing of the UCs must provide a space-filled construct, leads to a limit of the possible number of the SGS's: 230 all in all.

As for the point-group symmetries, for space-group notations there are the Hermann-Maguin (HM) notation, and Schoenflies (Sch) notation and. However, in the case of the space groups, the Sch notation is rarely used, and so we proceed only with the HM notation <sup>Note 3</sup>. Let us first see how to read these notations, and we take for that purpose we take cristobalite, a chiral  $\text{SiO}_2$  mineral. Its space group symmetry is described by the following notation:

**P4<sub>1</sub>2<sub>1</sub>2.**

The numbers in this notation are the symmetry elements of the UC molecular content. For cristobalite, these symmetry elements are three perpendicular rotational symmetry axes: two screw axes -  $4_1$  and  $2_1$ , and a 2-fold rotation axis. The order of the axes follows a hierarchy – the first position



is usually (but not always) assigned to the highest-order axis, 4 in our case <sup>Note 4</sup>. Being chiral, cristobalite appears in two different enantiomorphic crystals. Following the handedness notation explained in the previous section,  $P4_12_12$  is the space group of the right-handed mineral, and  $P4_32_12$  is of the left-handed one. As we shall see shortly, such notations of pairs of space group symmetries are possible only if they contain any of the  $3_1 - 3_2$ ,  $4_1 - 4_3$ ,  $6_1 - 6_5$ , and  $6_2 - 6_4$  roto-glide symmetry enantiomorphic elements.

Any other symbol of symmetry elements in the SGS notation - lower case letters, numbers with a minus sign or a macron - indicates an achiral crystal, even if it comes in combination with rotational symmetries. For example, sphalerite ((Zn,Fe)S), an achiral mineral, has the SGS notation of  $P\bar{4}3m$ , that is, a combination of rotational symmetry (3) with the achiral elements of roto-reflection symmetry ( $\bar{4}$ ) and mirror symmetry (m).

The first upper-case letter in the space-group notations refers to the lattice variety (primitive, P, for cristobalite). Mineral listings also routinely indicate the lattice-system - tetragonal in the case of cristobalite – but the practice is to attach the lattice variety (which together with the lattice system indicates one of the 14 Bravais lattices), to the list of symmetry elements. This distinguishes between space groups which contain the same symmetry elements but in different Bravais lattices. An example are the chiral crystals which have both 2-fold and 3-fold rotational symmetries (and only these symmetries), which appear in the space groups P23, F23, and I23 - all in the cubic lattice system - and in R32 in the trigonal lattice system. In any event and as already mentioned above, for a preliminary yes-no identification of chirality, the lattice-variety symbol can be ignored.

2.5.2. Chiral Crystals - Söhncke Space-Group Symmetries

Out of the crystallographic allowed 230 SGSs, 165 contain at least one improper symmetry element and are therefore describing achiral crystals (only) – these are the *improper-elements space groups*. The other 65 space groups contain only proper (rotational) symmetry elements - collectively known as *Söhncke group symmetries* (or proper or rotational space-groups). Following the above framed instruction of how to identify chirality, these 65 space groups are applicable for chiral crystals (only) – see Table 1, right column (the left columns is explained later on).

Table 1. The 65 Söhncke space groups symmetries.

<u>Crystal class</u> <u>and system</u> <sup>a</sup>	<u>Space group</u> <sup>b</sup>
1 ( $C_1$ ) Pedial Triclinic	P1 (#1)
2 ( $C_2$ ) Sphenoidal Monoclinic	P2 (#3), P2 <sub>1</sub> (#4), C2 (or A2, B2) (#5)
222 ( $D_2$ ) Rhombic-disphenoidal Orthorhombic	P222 (#16), P222 <sub>1</sub> (#17), P2 <sub>1</sub> 2 <sub>1</sub> 2 (#18), P2 <sub>1</sub> 2 <sub>1</sub> 2 <sub>1</sub> (#19), C222 <sub>1</sub> (#20), C222 (#21), F222 (#22), I222 (#23), I2 <sub>1</sub> 2 <sub>1</sub> 2 <sub>1</sub> (#24)
4 ( $C_4$ ) Tetragonal-pyramidal Tetragonal	P4 (#75), P4 <sub>2</sub> (#77), I4 (#79), I4 <sub>1</sub> (#80) P4 <sub>1</sub> (#76)/P4 <sub>3</sub> (#78)
422 ( $D_4$ ) Tetragonal-trapezohedral Tetragonal	P422(#89), P42 <sub>1</sub> 2(#90), P4 <sub>2</sub> 22 (#93), P4 <sub>2</sub> 2 <sub>1</sub> 2 (#94), I422 (#97), I4 <sub>1</sub> 22 (#98) P4 <sub>1</sub> 22 (#91)/P4 <sub>3</sub> 22 (#95), P4 <sub>1</sub> 2 <sub>1</sub> 2(#92)/P4 <sub>3</sub> 2 <sub>1</sub> 2 (#96)
3 ( $C_3$ ) Trigonal-pyramidal Trigonal	P3 (#143), R3 (#146) P3 <sub>1</sub> (#144)/P3 <sub>2</sub> (#145)
32 ( $D_3$ ) Trigonal-trapezohedral	P312 (#149), P321 (#150), R32 (#155) P3 <sub>1</sub> 12 (#151)/P3 <sub>2</sub> 12 (#153), P3 <sub>1</sub> 21 (#152)/P3 <sub>2</sub> 21 (#154)

Trigonal	
6 (C <sub>6</sub> )	P6 (#168), P6 <sub>3</sub> (#173)
Hexagonal-pyramidal	<b>P6<sub>1</sub> (#169)/P6<sub>5</sub> (#170), P6<sub>2</sub> (#171)/P6<sub>4</sub> (#172)</b>
Hexagonal	
622 (D <sub>6</sub> )	P622 (#177), P6 <sub>3</sub> 22 (#182)
Hexagonal-trapezohedral	<b>P6<sub>1</sub>22(#178)/P6<sub>5</sub>22 (#179), P6<sub>2</sub>22(#180)/P6<sub>4</sub>22(#181)</b>
Hexagonal	
23 (T)	
Tetartoidal	P23 (#195), F23 (#196), I23 (#197), P2 <sub>1</sub> 3 (#198), I2 <sub>1</sub> 3 (#199)
Cubic	
432 (O)	P432 (#207), P4 <sub>3</sub> 2 (#208), F432 (#209), F4 <sub>3</sub> 2 (#210), I432 (#211),
Gyroidal	I4 <sub>1</sub> 32 (#214)
Cubic	
	<b>P4<sub>3</sub>2 (#212)/P4<sub>1</sub>32 (#213)</b>

(a) 1st line: The Hermann-Maguin and (*Schoenflies*) notations of the symmetry class. 2nd line: The shape name of the symmetry class. 3rd line: The *Crystal system*. (b) The 11x2 enantiomorphic pairs are in **bold**. All others are the 43 non-enantiomorphic. (#space-group number).

The 65 Söhncke group symmetries are further sub-divided into two distinctly different SGS's: The first - **Söhncke enantiomorphic space groups** – are composed of the roto-glides 3<sub>1</sub>-3<sub>2</sub>, 4<sub>1</sub>-4<sub>3</sub>, 6<sub>1</sub>-6<sub>5</sub> and 6<sub>2</sub>-6<sub>4</sub>, alone or in combination with the other allowed rotational elements, (the identity (1), the two-fold (2), three-fold (3), four-fold (4) and six-fold (6) rotational symmetries), and all of which are in the primitive (P) lattice. There are 22 Söhncke space groups of this kind, which are actually 11 pairs of right (the lower m index) left-handed (the higher one) space-group pairs (11x2=22), and these are bolded in Table 1. An example is again cristobalite, which appears in nature as two enantiomorphic minerals in either the space groups P4<sub>1</sub>2<sub>1</sub>2 or the space group P4<sub>3</sub>2<sub>1</sub>2. For these 11 enantiomorphic pairs, the handedness labeling rule is simple and follows the accepted convention for helixes, as expressed by the roto-glides and explained above: right-handed cristobalite is P4<sub>1</sub>2<sub>1</sub>2 while left-handed cristobalite is P4<sub>3</sub>2<sub>1</sub>2.

The other (65-22=) 43 Söhncke space groups – Table 1 – contain, alone or in combinations, all rotational elements including the roto-glides 2<sub>1</sub>, 4<sub>2</sub>, and 6<sub>3</sub>, (but not 3<sub>1</sub>-3<sub>2</sub>, 4<sub>3</sub>, 6<sub>1</sub>-6<sub>5</sub> and 6<sub>2</sub>-6<sub>4</sub> which appear only in the 11 enantiomorphic space groups). They also contain the roto-glide 4<sub>1</sub> but only in non-primitive lattices. Since rotational elements and the roto-glides 2<sub>1</sub>, 4<sub>2</sub>, and 6<sub>3</sub> do not provide enantiomorphic information (Section 2.4, and so is 4<sub>1</sub> in non-primitive lattices) this sub-group of 43 are termed **Söhncke non-enantiomorphic space groups** <sup>Note 5</sup>. The inability of this sub-group to indicate handedness creates a problematic situation: For instance, although epsomite, MgSO<sub>4</sub>·7H<sub>2</sub>O, appears in nature as two distinctly different enantiomorphic minerals, the space group label of this mineral, P2<sub>1</sub>2<sub>1</sub>2<sub>1</sub>, is blind to that fact – we return to that issue in Section 5.4.

We can now re-phrase the above criterion of chirality, and tailor it directly to crystals:

A mineral is chiral if its space-group symmetry is one of the 65 Söhncke space groups.

Having the same space group symmetry for two chemically different crystals may indicate a similar molecular structure, but this is not necessarily so. For instance, cinnabar (HgS) and quartz (SiO<sub>2</sub>) are two chiral minerals in the enantiomorphic space groups P3<sub>1</sub>21 and P3<sub>2</sub>21, but their actual molecular structures – described in more detail below – are quite different: in HgS the 3<sub>1</sub> or 3<sub>2</sub> helixes are of -Hg-S- chains, while for quartz the helixes are of oxygen-linked SiO<sub>4</sub> tetrahedra. This, in fact, is an important fact to notice – *a given symmetry never provides full information of the specific details of the actual molecular arrangement*, but instead, provides a general shape descriptor. Yet, examples of crystals which share the same space group symmetry and also similar spatial arrangement of their different elements, exist and are referred to as **isostructural** crystals. Examples are berlinite (Al(PO<sub>4</sub>)) and quartz, both of the enantiomorphic space groups P3<sub>1</sub>21/P3<sub>2</sub>21, and both with tetrahedral building units - tetrahedral phosphate and the tetrahedral Si(OSi)<sub>4</sub> units. Likewise, chemically related minerals may appear as either isostructural crystals or as crystals of different space groups. These two

situations are exemplified with  $\text{GeO}_2$  minerals: The element Ge is just below Si in the periodic table, and while pertoldite, a  $\text{GeO}_2$  mineral, preserves the same space group and chirality of quartz (that is, quartz and pertoldite are isostructural), argutite, another  $\text{GeO}_2$  mineral, packs in the completely different achiral space group of  $P4_2/mnm$ .

## 2.6. The Asymmetric Unit

The symmetry elements that appear in the space group notation have also the role of telling us how to build the atomic and molecular structural content of the unit-cell (UC) from the smallest possible assembly of atoms inside it, by applying on that smallest assembly the symmetry operations indicated in the space group label. That smallest assembly of atoms from which the whole content of the UC is built is called the **asymmetric-unit** (AU). It may be a single atom, a molecular fragment, one or more monomeric units (formula units), a whole single molecule, and even as large as several molecules. Mineral listings contain also the Z and Z' numbers: Z is the number of molecules or formula units in the UC, while Z' is the number of molecules or formula units in the AU; they are the same if the AU is the whole content of the UC.

In crystallographic databases, usually only the coordinates of the atoms in the AU are provided - rather than the whole UC - from which the UC is then derived by applying the symmetry elements of the space group. For example, the AU of both right-handed and left-handed quartz is the small Si-O unit (The Structure of Materials, <http://som.web.cmu.edu/structures/S097-alpha-quartz.html>). From this diatomic AU, the UC which contains a helical chiral  $\text{Si}_3\text{O}_6$  assembly (three formula units of  $\text{SiO}_2$ ) (The Quartz Page, [http://www.quartzpage.de/gen\\_struct.html](http://www.quartzpage.de/gen_struct.html)), is constructed by applying on the Si-O the two rotational operations - either  $3_1$  for the right-handed enantiomorph, or  $3_2$  for the left-handed one - and 2, which appear in quartz space group notation,  $P3_121$  (the identity element, 1, sometimes appears explicitly in the space group notation). Note that quartz' AU, Si-O, is in fact achiral: it has mirror symmetry in the page plane and rotational  $C_{\infty}$  along the Si-O bond. Indeed, one should not be confused by the "asymmetric" in asymmetric unit: Asymmetry in this context means that the symmetry elements of the AU itself, do not take part in the space-group instructions of how to build the UC.

Let us generalize the observation that a chiral crystal - quartz - can be built from an achiral AU - Si-O: A chiral UC maybe built from either chiral or achiral AUs, provided that the only symmetry elements in the space group are rotational; and an achiral UC likewise can be built from either chiral or achiral AUs, provided that the space group contains at least one improper symmetry element such as reflection or (the very common) inversion. Wollastonite, ( $\text{CaSiO}_3$ ), is an example of a chiral AU leading to an achiral crystal - its SGS is  $P\bar{1}$ , that is, the UC has (achiral) inversion symmetry. The chiral AU of this mineral is composed of three helically oxygen-linked  $\text{SiO}_4$  tetrahedra -  $\text{Ca}_3\text{Si}_3\text{O}_9$  - but in the UC this AU is then linked to symmetry-inverted three opposite-twisting tetrahedra, for a total of an achiral assembly of 6 formula units (The Structure of Materials, <http://som.web.cmu.edu/structures/S092-wollastonite.html>).

Additional molecular building blocks are used in the description of crystals, particularly polyhedral units. Thus, we have seen that for silicates, the  $\text{SiO}_4$  tetrahedron is often used. In other oxides the tetrahedral  $\text{TT}'_4$  unit is used, which is the  $\text{T}(\text{O}-\text{T}')_4$  unit without the oxygen atoms, where T and T' are, e.g., Si, Al, Ti, etc.) (Yogev-Einot and Avnir, 2004; Dryzun et al, 2009). Another building block which is commonly used in the zeolites literature is the secondary building unit (SBU): The framework of the zeolite is divided into units, of up to 16 T atoms, without the oxygen atoms (Dryzun et al, 2009). When it comes to chiral crystals, all of these alternative building blocks are chiral as well, because a chiral environment always induces to some extent its chirality its own building blocks.

## 2.7. Conglomerates and Racemates

Solutions or melts from which (non-biological) chiral crystals form, contain a mixture of the molecular enantiomers, usually at a 1:1 ratio which is termed a **racemate** or a **racemic mixture**. In the case of chiral crystals which are based on conformational chirality of achiral molecules, the racemic situation refers to left- and right-handed chiral conformers, which are later captured in the crystal.

Such molecular solutions or melts have two optional routes of crystallization: The first is where each of the enantiomers crystallizes separately into its enantiomorphic crystal – in that case, a *conglomerate* of crystals will be obtained, where the left- and right-handed enantiomorphic crystals appear as a mixture of about 1:1 (note that this 1:1 situation is not termed “racemate” but conglomerate). The UCs of the components of a conglomerate are, likewise, enantiomorphic. Practically, most of the chiral minerals, belong to that category. The second option is that the two counter enantiomers of the molecule co-crystallize as pairs of left- and right enantiomers within the same UC. Inclusion of both enantiomers in the UC may lead to either an achiral crystal (no conglomerate form) or, again, to a conglomerate of chiral crystals. An achiral crystal is obtained when the pair of the opposite enantiomers are co-aligned within the UC with a mirror or inversion symmetric way (or in higher  $S_n$  symmetries). The AU in this case is one of the enantiomers (or a fraction of it) – and the counter enantiomer within the UC is obtained by applying on it the mirror or inversion symmetry operation, whichever appears in the space-group symmetry of that crystal. As the resulting achiral crystal is composed of a 1:1 ratio of the two opposite enantiomers, it is termed *racemic crystal* (or *heterochiral crystal*). The other less common situation of crystalizing the racemic solution as pairs of enantiomers, is that the pair is not aligned in a symmetrical way by one of the improper symmetry elements inside the UC (which would lead to achirality). In that situation, the AU comprises of the pair of the enantiomers, leading to a chiral crystal, and again to a conglomerate of enantiomorphs. Such chiral crystals are termed *kryptoracemates* (that is, a racemate which is hidden by the space group symmetry of the crystal (Fabian and Brock, 2010). The delicate point in that case is that the resulting chirality of the crystal is not because of the chirality of each of the enantiomers, but because of the way they are co-aligned in the UC <sup>Note 6</sup>.

### 3. The Chiral Minerals Found in Nature

#### 3.1. The Abundance of Chiral Minerals and the “Missing Glove” Situation

The abundance of specific chiral minerals, that is, minerals which are described by one of the 65 Söhncke space group symmetries, varies widely – from quartz, which makes 12% of the Earth's land surface, to rare chiral minerals such as the zeolitic goosecreekite (Dryzun, C. et al., 2009). Most of the chiral minerals are not common, and yet in terms of percentage of the total number of different minerals, they emerge as a family which deserves special attention: We show in this review that about 10% of all minerals – that is, close to 600, have been characterized as having a Söhncke space-group symmetry (see also (Dryzun, C., Avnir, D., 2012) for statistics of all non-biological crystals, where as high as 23% of chiral crystals was estimated). There are two main reasons for the considerable abundance of chiral minerals: First, we recall that in order to be achiral, the object *must* have a reflection symmetry or a higher improper symmetry. A requirement to have symmetry, is much more restrictive than the most elementary condition for having chirality, that is, not having any symmetry at all; true, chiral objects may have rotational symmetry, but that is not a requirement. And second, as explained above, conformational chirality which is the main source of chirality in minerals, offers endless molecular chiral architectures.

Despite the abundance of types of chiral minerals, in practice, many reports of minerals in the Söhncke space groups do not use the descriptor “chiral” at all, and lack an explicit recognition that two types of the specific mineral are possible – the two enantiomorphs. Likewise, identification of which of the two enantiomorphs is at hand, is usually missing; this is the “*missing-glove*” situation: Only one “glove” is reported, and often without identifying whether it is the left- or right-handed glove, or by assigning arbitrarily one of the two possible enantiomorphic space groups. The rare cases where the two enantiomorphs are described in the same report are listed below. An explanation for that neglect – besides not being always aware of the implication of chirality – is that the standard commercial “black-box” analytical tools of analysis of X-ray crystallographic data are not always tailored to distinguish between the left-handed and right-handed options - a practice termed the determination of the *absolute configuration* - and often one needs a more sophisticated data analyses by expert crystallographers (Section 6.2). Adding to that situation is the fact that while for the 11x2



enantiomorphic helical space groups, each enantiomorph has its own label, making the labeling of left- or right-handed minerals clear, there is no standardly agreed convention for labeling the handedness of crystals which reside in the 43 non-enantiomorphic Söhncke space groups, which anyway do not provide a space-group labeling distinction between the two enantiomorphs. Adding to the difficulty of identifying the chirality of minerals is the fact that, quite often, the macroscopic shape and form of chiral minerals – their habits (Section 5) - do not clearly reveal and reflect, if at all, the molecular-level enantiomorphism in two clear mirror-image related habits.

Another aspect of the missing glove situation is that reports usually refer to only one of the gloves – based on an arbitrarily selected crystal-species from the site – but the counter enantiomorphic glove is surely there. The ideal practice would have been to collect several samples from the mineral's site, analyze them all, and identify each of the two enantiomorphs. Indeed, the well-studied quartz and the several exceptions where the two enantiomorphs are reported following crystallographic analysis or by visual inspection of the habits show that, yes, the missing glove is always there to be identified – these examples are described in the next two sections.

### 3.2. Chiral Minerals in the 22 Enantiomorphic Space-Group Symmetries

We begin the description of the chiral minerals that belong to the 11x2 enantiomorphic space groups. There are 58 minerals that belong to that category, and are collected in Table 2. As explained above, in this family of chiral space groups, each pair of enantiomorphs has different space-group labels for the right-handed or left-handed versions, and the assignment of handedness follows the handedness labeling of the helical symmetry element within the space group: It is right-handed if it contains the roto-glide elements 3<sub>1</sub>, 4<sub>1</sub>, 6<sub>1</sub>, or 6<sub>2</sub>, and it the left-handed enantiomorph if it contains (in the same order) the elements 3<sub>2</sub>, 4<sub>3</sub>, 6<sub>5</sub>, 6<sub>4</sub>. Yet, because of the missing glove common situation described above, the chiral minerals listed in Table 2 are paired as belonging to either/or one of the two possible of enantiomorphic space groups (following a similar recommendation in (Urusov and Nadezhina, 2009); the cases where each of the two enantiomorphs has been identified, are bolded in that table, and are detailed next:

**Table 2.** Chiral minerals in the 22 enantiomorphic space-group symmetries.

\* The heavily studied, well characterized enantiomorphs of quartz (space-groups P3<sub>1</sub>21 and P3<sub>2</sub>21) has been reviewed (Götze, J. et al., 2021; The Quartz Page, <http://www.quartzpage.de/>), well characterized (Carretero-Genevri et al, 2015), and will continue to be mentioned in this review in various contexts.

\* Cinnabar, HgS, the most common source for mercury production, is of the same enantiomorphic space groups as that of quartz, P3<sub>1</sub>21 and P3<sub>2</sub>21. As seen in Table 2, this enantiomorphic pair of space groups is commonly found in many chiral minerals. The chirality of cinnabar is best manifested by the helical chains of -Hg-S-Hg-S-Ag-S-, which are either left-handed or right-handed. The two enantiomorphs of this mineral, obtained from various locations, were studied in detail by Shindo et al (Shindo et al, 2013). The two absolute helical handedness configurations were determined from X-ray single crystal structure analysis using the Flack parameter (described in Section 6.2). Note that these authors use the IUPAC approved labeling of the handedness of helicity – *P* for the right-handed P3<sub>1</sub>21 (not to be confused with the *P* for primitive lattice) and *M* for the left-handed P3<sub>2</sub>21 <sup>Note 7</sup>.

\* Cyrilovite, a phosphate mineral (NaFe<sub>3</sub><sup>3+</sup>(PO<sub>4</sub>)<sub>2</sub>(OH)<sub>4</sub>·2(H<sub>2</sub>O)) found in granitic pegmatites, has enantiomorphs in the space groups P4<sub>1</sub>2<sub>1</sub>2 and P4<sub>3</sub>2<sub>1</sub>2. This pair of space-groups is also quite common for chiral minerals (Table 2). The cyrilovite sample studied - here too, the handedness was assigned using Falck's methodology - was twinned as left-right pairs (Cooper et al, 2000) (we return to the twinning phenomenon in more detail in Section 5.2.2). Notice in Table 2 that not only is this phosphate chiral, but that chiral phosphate minerals are quite common in that list – some degree of deviation of the phosphate unit from prefect achiral tetrahedrality is, as mentioned above, expected

(Yogev-Einot and Avnir, 2007). Cyrilovite and two of the other chiral phosphates in the Table, are not only isostructural but also *isomorphous*, that is, not only that they share the same space-group and general structure (isostructural), but that they reflect a simple substitution of an ion: wardite,  $\text{NaAl}_3(\text{PO}_4)_2(\text{OH})_4 \cdot 2(\text{H}_2\text{O})$ , in which the iron in cyrilovite is replaced by aluminum, and fluorowardite,  $\text{NaAl}_3(\text{PO}_4)_2(\text{OH})_2\text{F}_2 \cdot 2\text{H}_2\text{O}$ , in which in addition, fluorine replaces two OH groups.

\* Particularly interesting chiral minerals are maghemite, spinel-structured  $\gamma\text{-Fe}^{+3}_2\text{O}_3$  (more accurately,  $\text{Fe}^{3+}_{0.67}\square_{0.33}\text{Fe}^{3+}_2\text{O}_4$ ) and its closely related titanomaghemite,  $(\text{Ti}^{4+}_{0.5}\square_{0.5})\text{Fe}^{3+}_2\text{O}_4$ , which, like (achiral) magnetite, are ferrimagnetic minerals, thus combining the properties of chirality and magnetism. Both minerals are of the enantiomorphic space groups  $P4_132$  and  $P4_332$ . The two enantiomorphic crystals of maghemite have been identified by electron microscopy in the same specimen as microscopic domains, although the assignment of which domain is “left” and which is “right” is arbitrary in these reports (Van der Biest and Thomas, 1975; Smith, 1979).

\* Two other interesting minerals in the enantiomorphic space groups are (the non-metal) selenium and (the metalloid) tellurium, two of the elements which appear in nature as minerals of the purely zero-valent form elemental. They are also the only elements in the periodic table which are chiral in their native forms. Selenium appears in several allotropes, the most stable and dense form of which is a (chiral) helix of Se atoms (three atoms per turn), and which packs in the enantiomorphic helical space groups  $P3_121$  and  $P3_221$  (again, as quartz). The same chiral structure characterizes the Te. Identification of enantiomorphic pairs of Se and Te appears in a number of publications on synthetic crystals of these elements (Kozlovskaya et al, 2023), but so far not on mineral sources, although, no doubt, they appear as pairs in nature as well.

### 3.3. Chiral Minerals in the 43 Non-Enantiomorphic Söhncke Space-Groups

Chiral minerals in the 43 non-enantiomorphic Söhncke space-groups abound, and are more common – about 470 minerals (Mindat listings) compared with 58 in the enantiomorphic space groups. Many of the non-enantiomorphic space-group chiral minerals are discussed, listed and mentioned throughout the text in the next Sections, and additional ones are collected in Table 3, to emphasize the highly diverse chemical composition types of these minerals in nature, across the space groups (see also (Lee et al, 2022, supplementary). Table 3 also collects the number of chiral minerals in each of the non-enantiomorphic space groups, to be discussed below. It is not surprising that there are many more chiral minerals in the non-enantiomorphic space groups, considering the larger number of the non-enantiomorphic space groups, which include also the non-restrictive  $P1$  space group. Minerals in the  $P1$  space group, we recall, lack molecular symmetry of their UC altogether – the only symmetry found here is the translational symmetry, forming the whole crystal. In this space group the molecular building blocks have higher freedom to acquire any conformation that minimizes the energy of the crystal. (The number of  $P1$  minerals is also probably higher, because of a common crystallographic difficulty to distinguish between this space group and the achiral  $P\bar{1}$ , which is the most common mineral space group (Webmineral, <http://webmineral.com/crystal/Triclinic.shtml>). The next most common space groups are  $P2_12_12_1$  with 51 representatives and  $P2_1$  with 50. In fact, these space groups are the most common packings of chiral crystals in general – organic, biological (Powder Diffraction on the WEB, <http://pd.chem.ucl.ac.uk/pdnn/symm3/sgpfreq.htm>) and inorganic (Urusov and Nadezhina, 2009) - even more than  $P1$  (Cambridge Structural Database, <https://www.ccdc.cam.ac.uk/media/CSD-Space-Group-Statistics-Space-Group-Number-Ordering-2024.pdf>). The question of why  $P2_12_12_1$  is of high frequency has occupied the literature for quite a while. An intuitive answer, given at least for proteins and which goes along the explanation given for  $P1$ , is that this space group (as well as  $P2_1$ ) are “less restrictive than others in that they allow the molecules more rigid-body degrees of freedom and can therefore be realized in a greater number of ways” (Wukovitz and Yeates, 1995). As is the case for  $P2_1$ , the next four common space groups contain only one symmetry element -  $P6_3$  (43 minerals),  $C2$  (31),  $R3$  (26),  $P3$  (26) – but this simplicity cannot serve as a general rule:  $P6$  is with only one reported chiral mineral, and  $P4$  with no reported minerals. In fact, 14 of the space groups have no representative at all, interestingly, most of which contain a 4-fold rotational symmetry axis.

**Table 3.** Chiral minerals in the 43 non-enantiomorphic space-group symmetries. Total numbers and representative minerals.

Several reports appeared, which describe the existence of two enantiomorphs:

\* Leucophanite,  $\text{NaCaBeSi}_2\text{O}_6\text{F}$ , crystallizes in the commonly found  $P2_12_12_1$  space group. The structural study of Friis et al (Friis and Balic-Zunic, 2005) is a good example of what one would wish to see much more, regarding chiral minerals: Nine samples were analyzed diffractometrically, and the structure solution revealed the existence of the two enantiomorphs, some of which were twinned. Labeling these as left or right followed the helicity sense of the corner-connected tetrahedral silicate chain which builds this mineral.

\* Epsomite,  $\text{MgSO}_4 \cdot 7\text{H}_2\text{O}$ , crystallizes in the  $P2_12_12_1$  group as well. An excellent historic account on the identification of two enantiomorphic habit forms of this mineral (as well as other properties of this mineral) appeared in (Fortes, 2020). Epsomite provides a nice example of isomorphism for the non-enantiomorphic chiral minerals: Replacing Mg with Zn provides goslarite,  $\text{ZnSO}_4 \cdot 7\text{H}_2\text{O}$ , and replacing with Ni provides morenosite,  $\text{NiSO}_4 \cdot 7\text{H}_2\text{O}$ , all of the same space group,  $P2_12_12_1$ .

\* Austinite,  $\text{CaZnAsO}_4(\text{OH})$ , is a third example in the common space-group  $P2_12_12_1$  and another example of identifying the two enantiomorphs by examination of the macroscopic habit (Staples, 1935; Williams and de Azevedo, 1967; Austinite, <https://en.wikipedia.org/wiki/Austinite>).

\* Nepheline,  $\text{Na}_3\text{KAl}_4\text{Si}_4\text{O}_{16}$ , is a chiral magmatic mineral in the space group  $P6_3$ . The two enantiomorphs detected in this study were identified from the microscopic shapes of HCl-etching features – left-handed and right-handed etched features were clearly identified (Hejl and Finger, 2018). The etching methodology has been used also for identification of the enantiomorphs of quartz (Wilson, 1979; Gault, 1949).

\* Petzite,  $\text{Ag}_3\text{AuTe}_2$ , crystallizes in the space group  $I4_132$  (which is not an enantiomorphic space group, despite the 4<sub>1</sub> element – Section 2.5.2). The study of Hongu et al who determined it (Hongu et al, 2019) is mentioned here to highlight the unsolved issue of handedness labeling: Although these authors report only one of the two enantiomorphs, the handedness of that mineral has been a central issue. The absolute handedness was determined by analyzing the crystallographic data using Flack parameter, and they discuss previous reports, questioning the handedness assignment there: “The opposite configuration reported previously may therefore have simply been the result of an arbitrary assignment.” The authors also refrain from assigning the label “left” or “right” to the enantiomorph they isolated, and just show the mirror non-superimposable image of the unite cell. That practice is recommended in the absence of a clear, simple handedness convention which can be assigned straightforwardly to the studied mineral (Hongu et al, 2019).

\* Kaolinite,  $\text{Al}_2\text{Si}_2\text{O}_5(\text{OH})_4$ , a very abundant mineral, crystallizes in the most common space group of chiral minerals,  $P1$ . Usually, kaolinite appears as a conglomerate of left- and right-handed crystals of equal amounts, and these were identified by shape-analysis of nanocrystals using microscopy (Samotoin, 2011). Lacking a methodology for handedness labeling, the selection of which of the enantiomorphs was labeled left, and which right, appears to be arbitrary. Of the 80 minerals which crystallize in this  $P1$  symmetry, apparently no enantiomorphic pairs have been reported, except for kaolinite.

Finally, we return now to the observation that many reported minerals in the Söhncke space groups do not even mention that the mineral is chiral (and should exist therefore in two forms). An example is the small but unique family of chiral silicate zeolite minerals, all of which belong to the 43 non-enantiomorphic space-groups, and none of which is described as chiral; these are:

Chiral silicate zeolite minerals

Alflarsenite,  $\text{NaCa}_2\text{Be}_3\text{Si}_4\text{O}_{13}(\text{OH}) \cdot 2\text{H}_2\text{O}$ ,  $P2_1$

Amicite,  $\text{K}_2\text{Na}_2\text{Al}_4\text{Si}_4\text{O}_{16} \cdot 5\text{H}_2\text{O}$ ,  $I2$

Analcime,  $\text{Na}(\text{AlSi}_2\text{O}_6) \cdot \text{H}_2\text{O}$ ,  $P1$

Bikitaite,  $\text{LiAlSi}_2\text{O}_6 \cdot \text{H}_2\text{O}$ ,  $P1$

Edingtonite,  $\text{Ba}(\text{Al}_2\text{Si}_3\text{O}_{10}) \cdot 4\text{H}_2\text{O}$ ,  $P2_12_12$

Gismondine-Sr,  $\text{Sr}_4(\text{Si}_8\text{Al}_8\text{O}_{32}) \cdot 9\text{H}_2\text{O}$ , C222<sub>1</sub>

Goosecreekite,  $\text{Ca}(\text{Al}_2\text{Si}_6\text{O}_{16}) \cdot 5\text{H}_2\text{O}$ , P2<sub>1</sub>

Hsianghualite,  $\text{Ca}_3\text{Li}_2(\text{Be}_3\text{Si}_3\text{O}_{12})\text{F}_2$ , I4132

Nabesite,  $\text{Na}_2\text{BeSi}_4\text{O}_{10} \cdot 4\text{H}_2\text{O}$ , P2<sub>1</sub>2<sub>1</sub>2<sub>1</sub>

Pahasapaite,  $\text{Li}_8(\text{Ca}, \text{Li}, \text{K})_{10.5}\text{Be}_{24}(\text{PO}_4)_{24} \cdot 38\text{H}_2\text{O}$ , I23

Ignoring the chirality of zeolites is somewhat surprising because when it comes to synthetic zeolites, their chirality is a main issue in many applications, including enantioselective catalysis, enantiomers separation, and more (Huang et al, 2024).

### 3.4. Chiral Organic and Carbonate Minerals

Minerals built from organic components are rare, basically because of the relative instability of these compounds to elevated temperatures and to oxidation processes. Yet, special attention has been given to this rare family of minerals, especially by Hazen et al (Carbon Mineral Challenge, [https://en.wikipedia.org/wiki/Carbon\\_Mineral\\_Challenge](https://en.wikipedia.org/wiki/Carbon_Mineral_Challenge); Hazen, 2019; Hazen et al, 2016), with the message that many more organic minerals do exist in nature, still waiting to be earthed. We believe this is true, even only because inorganic molecules are a small fraction of the total number of molecules on the surface of planet Earth, the majority of which are (bio)organic molecules. As already explained above, if a mineral is based on an inherently chiral biomolecule, then, since this molecule is single-handed in nature, we have the unusual situation of a chiral mineral for which only one of the enantiomorph exists – that of the naturally occurring biomolecule. Examples include:

\* Fichtelite (Strunz, H., 1962; Mace and Peterson, 1995), a purely hydrocarbon mineral,  $\text{C}_{19}\text{H}_{34}$ , a diterpene derivative 18-norabietane, which crystallizes in P2<sub>1</sub>. The single enantiomer of fichtelite is left-handed (S, by the CIP rules, as indicated in its IUPAC name, (1S,4aS,4bS,7S,8aS)-1,4a-dimethyl-7-(propan-2-yl)tetradecahydrophenanthrene.

\* Branchite (also known as hartite), is another diterpene hydrocarbon derivative,  $\text{C}_{20}\text{H}_{34}$ , (+)-phyllocladane ((1R,4S,9S,10R,13S,14S)-5,5,9,14-tetramethyltetracyclo[11.2.1.01,10.04,9]hexadecane) (Bouska et al, 1998). It crystallizes in space group P1.

\* Refikite,  $\text{C}_{20}\text{H}_{32}\text{O}_2$  ( $\text{C}_{19}\text{H}_{31}\text{COOH}$ ), the diterpenoid acid derivative related to abietenoic acid (see Pažout et al, 2018) for details) which crystallizes in P2<sub>1</sub>2<sub>1</sub>2 (mindat) or P2<sub>1</sub>2<sub>1</sub>2<sub>1</sub> (webmineral).

\* Dinite,  $\text{C}_{20}\text{H}_{36}$ , is the diterpenoid (13 $\alpha$ )-pimarane (4aR,4bS,7S,8aS,10aS)-7-ethyltetradecahydro-1,1,4a,7-tetramethylphenanthrene), which crystallizes in P2<sub>1</sub>2<sub>1</sub>2<sub>1</sub>.

All four are diterpenoid derivatives, and all four were discovered in fossilized wood environments. Indeed, this family of molecules is commonly found in wood. Unlike these four single enantiomer biomolecules which must lead to single mineral enantiomorphs, if the biomolecule is achiral but leads to a chiral crystal (conformational chirality), then the two enantiomorphs should exist in nature. Examples are:

\* Oxammite, a mineral which is the ammonium salt of oxalic acid,  $(\text{NH}_4^+)_2((\text{HCOO}^-)_2) \cdot \text{H}_2\text{O}$ , which crystallizes in P2<sub>1</sub>2<sub>1</sub>2.

\* Formicaite,  $\text{Ca}(\text{HCOO})_2$ , the Ca salt of two formic acid molecules, which was reported to crystallize in P4<sub>1</sub>2<sub>1</sub>2 (and so the enantiomorph P4<sub>3</sub>2<sub>1</sub>2 is also expected to be at the same site).

\* Ravatite,  $\text{C}_{14}\text{H}_{10}$ , is a mineral composed of pure phenanthrene, an aromatic polycyclic hydrocarbon, at space group P2<sub>1</sub>. Ravatite is a nice example of positional chirality (Section 2.3): Two molecules, planar and achiral, are placed in the UC in a helical chiral arrangement (Petríček et al, 1990).

\* Triazolite,  $\text{NaCu}_2(\text{N}_3\text{C}_2\text{H}_2)_2(\text{NH}_3)_2\text{Cl}_3 \cdot 4\text{H}_2\text{O}$ , the  $\text{Cu}^{2+}$  complex the 1,2,4-triazolate anion with an ammonia molecule as an additional ligand, crystallizing in P2<sub>1</sub>2<sub>1</sub>2<sub>1</sub>.

Although carbonate minerals are not usually categorized as organic, the carbonate anion is a key component in biogeochemical processes, particularly calcium and magnesium carbonates (Erez 2003; Hazen, 2019), and so we list the chiral carbonates in this Section as well. The simplest is monohydrocalcite,  $\text{CaCO}_3 \cdot \text{H}_2\text{O}$ , P3<sub>1</sub>21/ P3<sub>2</sub>21, but one can see that the majority are multiple cations-anions minerals. The most common type is the carbonate-silicate sub-family. This richness is due to



the conformational flexibility of the silicate building blocks, provides many possible conformers in the crystalline state – we return to this point in Section 4.3.

#### Chiral carbonate minerals

Alicewilsonite-(YCe),  $\text{Na}_2\text{Sr}_2\text{YCe}(\text{CO}_3)_6 \cdot 3\text{H}_2\text{O}$ , P1 (and related carbonates), P1  
 Balliranoite,  $(\text{Na},\text{K})_6\text{Ca}_2(\text{Si}_6\text{Al}_6\text{O}_{24})\text{Cl}_2(\text{CO}_3)$ , P6<sub>3</sub>  
 Britvinite,  $[\text{Pb}_7(\text{OH})_3\text{F}(\text{BO}_3)_2(\text{CO}_3)] [\text{Mg}_{4.5}(\text{OH})_3(\text{Si}_5\text{O}_{14})]$ , P1  
 Bussenite,  $\text{Na}_2\text{Ba}_2\text{Fe}^{2+}\text{Ti}(\text{Si}_2\text{O}_7)(\text{CO}_3)(\text{OH})_3\text{F}$ , P1  
 Cancrinite,  $(\text{Na},\text{Ca},\square)_8(\text{Al}_6\text{Si}_6\text{O}_{24})(\text{CO}_3,\text{SO}_4)_2 \cdot 2\text{H}_2\text{O}$ , P6<sub>3</sub>  
 Chiyokoite,  $\text{Ca}_3\text{Si}(\text{CO}_3)[\text{B}(\text{OH})_4]\text{O}(\text{OH})_5 \cdot 12\text{H}_2\text{O}$ , P6<sub>3</sub>  
 Depmeierite  $\text{Na}_8(\text{Al}_6\text{Si}_6\text{O}_{24})(\text{PO}_4,\text{CO}_3)_{1-x} \cdot 3\text{H}_2\text{O}$  ( $x < 0.5$ ) P6<sub>3</sub>  
 Donnayite-(Y),  $\text{NaCaSr}_3\text{Y}(\text{CO}_3)_6 \cdot 3\text{H}_2\text{O}$ , P1  
 Hanjiangite,  $\text{Ba}_2\text{CaV}^{3+}\text{Al}(\text{H}_2\text{AlSi}_3\text{O}_{12})(\text{CO}_3)_2\text{F}$ , B2  
 Huntite,  $\text{Mg}_3\text{Ca}(\text{CO}_3)_4$ , R32  
 Kyanoxalite,  $\text{Na}_7(\text{Al}_{6-x}\text{Si}_{6+x}\text{O}_{24})(\text{C}_2\text{O}_4)_{0.5+x} \cdot 5\text{H}_2\text{O}$  ( $0 < x < 0.5$ ), P6<sub>3</sub>  
 Latiumite,  $(\text{Ca},\text{K})_4(\text{Si},\text{Al})_5\text{O}_{11}(\text{SO}_4,\text{CO}_3)$ , P2<sub>1</sub>  
 Lecoqite-(Y),  $\text{Na}_3\text{Y}(\text{CO}_3)_3 \cdot 6\text{H}_2\text{O}$ , P6<sub>3</sub>  
 Monohydrocalcite,  $\text{CaCO}_3 \cdot \text{H}_2\text{O}$ , P3<sub>1</sub>21/ P3<sub>2</sub>21  
 Molybdophyllite,  $\text{Pb}_8\text{Mg}_9[\text{Si}_{10}\text{O}_{28}(\text{OH})_8\text{O}_2(\text{CO}_3)_3] \cdot \text{H}_2\text{O}$ , B2  
 Plumbotsumite,  $\text{Pb}_{13}(\text{CO}_3)_6(\text{Si}_{10}\text{O}_{27}) \cdot 3\text{H}_2\text{O}$ , C2 2 2<sub>1</sub>  
 Quintinite,  $\text{Mg}_4\text{Al}_2(\text{OH})_{12}\text{CO}_3 \cdot 3\text{H}_2\text{O}$ , P6<sub>3</sub>22  
 Slyudyankaite,  $\text{Na}_{28}\text{Ca}_4(\text{Si}_{24}\text{Al}_{24}\text{O}_{96})(\text{SO}_4)_6(\text{S}_6)_{1/3}(\text{CO}_2) \cdot 2\text{H}_2\text{O}$ , P1  
 Surite,  $(\text{Pb},\text{Ca})_3(\text{Al},\text{Fe}^{2+},\text{Mg})_2((\text{Si},\text{Al})_4\text{O}_{10})(\text{CO}_3)_2(\text{OH})_2$ , P2<sub>1</sub>  
 Thaumassite,  $\text{Ca}_3(\text{SO}_4)[\text{Si}(\text{OH})_6](\text{CO}_3) \cdot 12\text{H}_2\text{O}$ , P6<sub>3</sub>  
 UM2009-23-SiO:AlCCaClHKNaS,  $(\text{Na},\text{Ca})_{24}\text{K}_{10}[(\text{Si},\text{Al})_{60}\text{O}_{120}](\text{SO}_4)_{5.6}\text{Cl}_{1.5}(\text{CO}_3)_{0.4} \cdot 11\text{H}_2\text{O}$ , P3  
 Vishnevite,  $(\text{Na},\text{K})_8(\text{Al}_6\text{Si}_6\text{O}_{24})(\text{SO}_4,\text{CO}_3) \cdot 2\text{H}_2\text{O}$ , P6<sub>3</sub>  
 Weloganite,  $\text{Na}_2(\text{Sr},\text{Ca})_3\text{Zr}(\text{CO}_3)_6 \cdot 3\text{H}_2\text{O}$ , P1  
 Wyartite,  $\text{CaU}^{5+}(\text{UO}_2)_2(\text{CO}_3)_4(\text{OH}) \cdot 7\text{H}_2\text{O}$ , P2<sub>1</sub>2<sub>1</sub>2<sub>1</sub>.

### 3.5. Chiral Polymorphic Phase-Transitioned Minerals

We recall that **polymorphism** is the phenomenon of having for the same chemical compound various types of packing into a crystalline (or amorphous (Poole et al, 1995) form. A common source of inducing polymorphism in minerals are phase transitions affected by changes in temperature and pressure, either separately or combined.

One of the richest families of mineral polymorphs – both chiral and achiral - is that of silica,  $\text{SiO}_2$ , and so we use here this family (Drees et al, 1989) for the description of the chiral mineral polymorphism phenomenon in general. There are four chiral polymorphs of silica: quartz (P3<sub>1</sub>21/P3<sub>2</sub>21), cristobalite and keatite (rare) - both of which belong to the space groups P4<sub>1</sub>2<sub>1</sub>2/P4<sub>3</sub>2<sub>1</sub>2 - and tridymite, which is a chiral polymorph in the non-enantiomorphic space group C222<sub>1</sub>. The full picture of silica polymorphism includes also several achiral polymorphs, which are stishovite (P4<sub>2</sub>/mm), moganite (I2/a), coesite (2/m) and seifertite (Pbcn or Pb2n; found only in Lunar and Martian meteorites). Yet another achiral polymorph is the totally melted liquid phase, which leads to pure silica glass when cooled fast enough (see more about it in the next Section 4). Overall, the three primary polymorphs of silica – quartz, cristobalite and tridymite - are all chiral, quite a unique feature in the minerals' world. Specific polymorphs are stable at their characteristic temperature/pressure ranges, traditionally presented in the well-known **phase diagrams**, which include the liquid melt, the polymorphs (= solid phases), and the gas phase. From the thermodynamic point of view, only quartz is stable at room-temperature/atmospheric pressure, while all other polymorphs – chiral and achiral - are metastable under these conditions and stable at higher temperatures or pressures. However, these metastable phases are kinetically stable solids at room temperature/atmospheric pressure (and therefore listed by IMA as minerals).

The polymorphs picture gets even richer by the phenomenon of alpha (lower temperature) and beta (higher temperature) polymorphism. In the silica family, this kind of polymorphism exists for

quartz, cristobalite and tridymite. A well-known alpha-beta polymorph phase transition is that of quartz, where the common quartz – alpha quartz ( $P3_121/P3_221$ ) - converts to the high temperature beta-quartz (high-quartz) polymorph, which retains the chirality although at a different enantiomorphic space group,  $P6_222/P6_422$ . Beta-quartz is stable only above the transition temperature of  $573^\circ\text{C}$  (at atmospheric pressure), and cooling it leads back to alpha quartz; thus, beta-quartz is an example of a chiral mineral which exists only at high-temperatures. (For that reason, beta-quartz is not considered a formal mineral species by the IMA, which requires room-temperature stability, and so are the other beta polymorphs described next).

Cristobalite and tridymite undergo alpha-beta transitions as well (cristobalite at  $\sim 220^\circ\text{C}$  and tridymite at  $460^\circ\text{C}$ ), but, unlike quartz, in these two cases the transitions are between chiral and achiral polymorphs, that is, between the chiral alpha phases (cristobalite:  $P4_12_12/P4_32_12$ , tridymite:  $C222_1$ ) and the achiral high temperature beta phases (beta cristobalite:  $Fd\bar{3}m$ ; beta tridymite:  $P6_3/mmc$ ). Alpha – beta polymorphism is known also for other chiral minerals: Berlinite,  $\text{Al}(\text{PO}_4)$ , is isostructural with quartz, and interestingly, like quartz has also a similar alpha-beta transition (Ng and Calvo, 1976). Yet another example is alpha-cinnabar,  $\text{HgS}$ ,  $P3_121/P3_221$ ) and its high-temperature polymorph, beta-cinnabar (metacinnabar), for which chirality is lost ( $F\bar{4}3m$ ).

The richness of silica chiral crystalline polymorphic phases goes even greater considering the crystalline variations of the polymorphs themselves, known as *polytypes*. While polymorphs differ in their structural units (although all have the same molecular formula), polytypes, a subdivision of polymorphs, are minerals that differ from each other another only in the stacking of the same structural elementary unit which characterizes the polymorph. This is the case for tridymite which can occur - in addition to the alpha and beta crystal phases - as five additional polytypes, three of which are chiral: The high temperature ( $400^\circ\text{C}$ ) LHP polytype  $P6_322$ , the OP polytype ( $155^\circ\text{C}$ ,  $C222_1$ ), and the MX room temperature polytype, which is at the lowest (chiral) symmetry of  $C1$  (Tridymite, <https://en.wikipedia.org/wiki/Tridymite>). Changes of chirality/achirality within polytypes are found also with other chiral minerals, and examples are (chiral) kaolinite ( $P1$ ), which has three achiral polytypes: dickite, alloysite and nacrite (Kaolinite Subgroup, <https://www.mindat.org/min-43755.html>), all in space group  $Cc$ , and gersdorffite,  $\text{NiAsS}$ , which appears as three polytypes: the chiral gersdorffite,  $P2_13$ , and the two achiral ones, gersdorffite,  $Pa3$ , and gersdorffite- $Pca2_1$  (Bayliss, 1982).

Phase transitions between polymorphs may involve either cleavage and formation of new bonds (termed *reconstructive transformation*), or rearrangement of bond angles (and changes in bond lengths) with no bond cleavage (termed *displacive transformation*). The transition between quartz and tridymite is an example of the former (transition of the 3D molecular structure of quartz to the 2D layered structure for tridymite (Dapiaggi et al, 2015), and the alpha-beta silica polymorphs transition is an example of the latter (Hatch and Ghose, 1991). Likewise, displacive are the transitions between polytypes, since they involve only packing rearrangement of the same building block. In any event, phase diagrams should be treated with caution with regard to the actual reversible transition route between two neighboring phases, lying on either side of the equilibrium line which separates them. Thus, while for displacive transformations such as the chiral alpha-beta transitions, the separating line usually indeed represents direct transition between the two chiral phases, for reconstructive transformation the route leading for one to the other maybe quite complex and indirect, involving several steps (Overview of Silica Polymorphs, [http://www.quartzpage.de/gen\\_mod.html](http://www.quartzpage.de/gen_mod.html)). For instance, although beta-quartz and tridymite are neighboring phases, the transition between them is indirect - see ( $\beta$ -Tridymite, <https://www.mindat.org/min-47886.html>) for details.

Finally, note that from the handedness point of view there are several options in chiral phase diagrams. The common one should be that each of the chiral phases represents equal amounts of the right- and left-handed polymorphs (a conglomerate). The process of phase transition in this case means that each of the polymorphs either preserves the handedness or flips it at random. Phase transitions of which retains single handedness (left-phase-1 to either left-phase-2 or to a right-handed phase) are in principle possible in displacive transformations. These aspects of chiral crystals are quite unexplored, and certainly deserves attention.

## 4. Formation and Transformations of Chiral Minerals

### 4.1. Crystallization from the Melt

For sake of continuation with the previous section on chiral polymorphs, we begin Section 4 with the formation of crystals by liquid-solid phase transitions, that is, crystallization from the melt. We recall that when the melted liquid phase is cooled rapidly, the glass polymorph forms. For instance, in the silica family minerals, such glasses, *mineraloids* – for instance, lechatelierite and fulgurite – are obtained when crystalline silica minerals melt by high energy processes, such as a lightning strike, followed by rapid cooling. Other energetic events that convert crystalline silicates to glass include volcanic ejections and meteoritic impacts producing silica tektite droplets. In general, glass formation from chiral crystals, may result in either loss of chirality or in its retention. Loss of chirality occurs if the origin of the chirality in the crystalline state is conformational. In this case, rapid freezing results in a mixture of conformers (of varying low molecular weights in the case of polymeric minerals such as quartz), some of which are the racemates of chiral conformers, and hence, the glass is achiral. However, if the molecular building blocks of the crystal are of inherent chirality (which cannot conformationally invert), such as is the case for some bio-organic chiral minerals, the glassy melt will be chiral as well. However, the vast majority of glassy mineraloids result from the first option, and are achiral.

Slower cooling profiles of the melt give rise to crystallization, starting with the formation of nanocrystals at the interface with the outer colder environment. Depending of the cooling rate, the process may end in a solid which is a glass embedded with small crystals (*nanoliths*, *microlyths*, etc.). In other words, the lines in the phase diagram that separate the melt phase from the solids is actually never ideally infinitely thin, but has thickness representing a mixing of the two neighboring phases. In practice, if the melt originated from a conformational chiral mineral, then the back-crystallization of the melt into small crystalline seeds, should lead to equal amount of left- and right-handed embedded small crystals, regardless of whether the original crystalline source was a single-handed crystal, or a conglomerate of left and right-handed crystals. Therefore, such crystalline-seeded bulk glasses should not display physical properties related to chirality – such as optical rotation – although they should display chiral properties within the very short-range of a single nano or microcrystalline small phase. Indeed, glasses which are partially with dispersed crystallinity, have been treated in terms of *short-range order* materials with typical correlation lengths – see (Drewitt et al, 2022) for details. That being said, the possibility that an initial fluctuation in the crystallization process, will form an excess of one of the polymorphs, which then drags the entire system to a pure enantiomorphic excess, cannot be ruled out – this is rare in the melt, but has been reported in crystallizations from solution (Ward et al, 2010) although not, to the best of my knowledge, for minerals.

The exact composition of the partially crystalized glass from the point of view of which crystalline polymorphs form, and what is the size of the inclusions – from nanometers to centimeters and more - depends on the cooling rate and on other chemical components (in the case of cooling of a magma). High silica glassy igneous rocks which contain also silica-crystalline phases, are rich in cristobalite and quartz (Glassy igneous rock, <https://www.mindat.org/min-50714.html>), but contain mixtures of the enantiomorphs, and are therefore expected to be achiral. A well-known example which has accompanied humanity from prehistoric times, is obsidian glass, obtained mainly by rapid cooling of lava, which freezes crystalline inclusions of the high-temperature stable silica minerals such as the chiral cristobalite, most probably both enantiomorphs of it (The Mineral Cristobalite, <https://www.minerals.net/mineral/cristobalite.aspx>) inside the silica rich glass. Similarly, rhyolite and dacite, highly silica rich volcanic rocks, contain crystalline quartz as well, again, most probably both enantiomorphs of it.

For completion of this section, we also mention that crystalline minerals can from also form the vapor phase. A relevant example for this review is the precipitation of cristobalite form the vapor phase of eruptions from silicic volcanoes (Horwell et al, 2013).

### 4.2. Chirality Aspects of Crystallization of Minerals from Aqueous Solutions

The second main route of minerals formation are crystallizations and precipitations from aqueous solutions. These are affected by conditions that drive the concentrations of the relevant cations and anions above the solubility product constant of the specific mineral, which in turn are affected by the temperature of the aqueous solution, by its pH, by the rate of its evaporation (leading to evaporites), by the rate at which the relevant ions are replenished or are dissolved from mother minerals into the solution, by other solutes, and so on. It is a complex process, because quite often the small concentrations of impurity ions and other impurities, affect both the relevant chemical reaction and the crystallization. Here we focus on two main aspects of the crystallization of chiral minerals, namely the formation of hydrates and the formation of solid solutions.

Due to the common aqueous environment in which minerals form, quite often, the resulting crystal structure includes water molecules, the *hydrates* – we have seen many examples of chiral mineral hydrates in Tables 2,3 and Section 3. As these water molecules comprise an integral part of the UC, the details of the space-group symmetry refer to them as well. Thus, inclusion or removal of water molecules from the crystal, that is, changing the degree of hydration (the number of water molecules in the chemical formula), greatly affects the chirality/achirality of the crystal. Three minerals exemplify this point: The first is calcite ( $\text{CaCO}_3$ ), an achiral mineral (space group  $R\bar{3}c$ ; its common polymorph, aragonite, is achiral as well -  $Pmcn$ ), but the inclusion of one water molecule in the crystal induces chirality, forming (the less common) monohydrocalcite,  $\text{CaCO}_3 \cdot \text{H}_2\text{O}$ , with two enantiomorphs at space-groups  $P3_121$  and  $P3_221$ ). The next example, again of hydrates of a calcium mineral, are the hydrates of  $\text{CaCl}_2$ : Antarcticite,  $\text{CaCl}_2 \cdot 6\text{H}_2\text{O}$ , is a chiral mineral in space group  $P321$ , but crystallization with 4 water molecules, results in the achiral  $\text{CaCl}_2 \cdot 4\text{H}_2\text{O}$ ,  $P\bar{1}$ . Our third example is of the same trend, namely a chiral mineral which is heavily hydrated – epsomite,  $\text{MgSO}_4 \cdot 7\text{H}_2\text{O}$ , ( $P2_12_12_1$ ) - loses its chirality in minerals which are less hydrated, such as kieserite,  $\text{MgSO}_4 \cdot \text{H}_2\text{O}$  ( $C2/c$ ), starkeyite,  $\text{MgSO}_4 \cdot 4\text{H}_2\text{O}$  ( $P2_1/b$ ) and meridianiite,  $\text{MgSO}_4 \cdot 11\text{H}_2\text{O}$  ( $P\bar{1}$ ).

The second key phenomenon of crystallization we comment on, is the formation of *solid solutions*: If crystallization occurs in solution environments which contain different replaceable ions, then a crystal mineral may form, which includes various proportions of these replaceable ions, resulting in a crystal which is termed a solid solution. In general, a solid solution crystal, preserves its symmetry and chirality. For instance, one of the isomorphism cases described in Section 3, was that of epsomite, goslarite, and morenosite, all of which are  $P2_12_12_1$  structures of the the general formula  $\text{MSO}_4 \cdot 7\text{H}_2\text{O}$ , where M is one of the three similar divalent cations of Mg, Zn and Ni, respectively. These three minerals form in environments that are rich in one of the respective cations, lacking the other two. However, in aqueous environments where two or even three of these cations co-exist in various proportions, they may enter the  $\text{MSO}_4 \cdot 7\text{H}_2\text{O}$  skeleton at random (and hence the term “solution”), producing a solid-solution crystal which preserves its chirality and handedness.

### 4.3. Polymerizations Leading to Chiral Minerals

#### 4.3.1. The Silicates

Polymerization of small monomeric or oligomeric units leading to minerals, takes place either in the melts or in aqueous environments. The polymerization process is particularly common in the formation of silicate minerals, which are the largest family of minerals. The high richness of this family is not so much due to the abundance of the Si and O elements on Earth crust, but mainly due to the following parameters: First, the conformational freedom of the  $-\text{Si}-\text{O}-\text{Si}-$  unit, which includes rotation around the Si-O bonds and varying the Si-O-Si bonds angle (and to a lesser degree, the Si-O stretching), leading to a large variety of stable structures. From the energy-map point of view, one can envisage a landscape full of local wells, each representing such a stable silicate structure. Second, the silicates are anionic, and their conformational flexibility allows them to optimize a conformer which perfectly accommodates the counter cations as dictated by their size and charge. Third, adding to the conformational flexibility is the fact that the elementary monomeric building block, silicic acid ( $\text{Si}(\text{OH})_4$ ), has four Si-OH reactive arms, opening structures possibilities in 1D, 2D and 3D. The polymerization takes place with either silicic acid or with small oligomers of it (linear, branched or cyclic) and the reaction is typically a polycondensation, releasing water molecules. The monomers



and small oligomers that polymerize are obtained, for instance, by aqueous weathering and hydrothermal processes of silica-rich rocks such as basalt and various types of volcanic glass and volcanic deposits (such as pumice), and is particularly efficient where hot water can percolates through pores and cracks of these sources.

The architectures thus obtained start from small units including discrete single silicate units (orthosilicates or nesosilicates), dimers of that unit (sorosilicates), cyclic ring units (cyclosilicates), and increases to polymers of 1D structure (single chains and double-chain ladder, the inosilicates), 2D sheets (phyllosilicates), and plenty of 3D structures (tectosilicates). All of these silicate types have chiral minerals. An example of a chiral small unit silicate mineral is Sillénite,  $\text{Bi}_{12}\text{SiO}_{20}$ , of space group  $I23$ , which constitutes of discrete  $\text{SiO}_4$  tetrahedra, separated by a Bi-O framework. Of the three polymeric types, the richest family is that of the chiral and achiral tectosilicates, and this is so because of the larger number of possible conformational packings in 3D structures. Indeed, all of the chiral silicates listed so far in the other parts of this review are tectosilicates. Here are some examples of chiral silicate polymers of the other two families:

#### Chiral inosilicates

Frankamenite,  $\text{K}_3\text{Na}_3\text{Ca}_5(\text{Si}_{12}\text{O}_{30})[\text{F},(\text{OH})]_4 \cdot (\text{H}_2\text{O})$ ,  $P1$

Leucophanite,  $\text{NaCaBeSi}_2\text{O}_6\text{F}$ ,  $P2_12_12_1$

Taikanite,  $\text{Sr}_3\text{BaMn}^{2+}_2(\text{Si}_4\text{O}_{12})\text{O}_2$ ,  $B2$

,

Tobermorite,  $\text{Ca}_5\text{Si}_6\text{O}_{16}(\text{OH})_2 \cdot 4\text{H}_2\text{O}$  or  $\text{Ca}_4\text{Si}_6\text{O}_{17}(\text{H}_2\text{O})_2 \cdot (\text{Ca} \cdot 3\text{H}_2\text{O})$ ,  $C222_1$  or  $P2_1$

Umbite,  $\text{K}_2(\text{Zr,Ti})\text{Si}_3\text{O}_9 \cdot \text{H}_2\text{O}$ ,  $P2_12_12_1$

#### Chiral phyllosilicates

Britvinite,  $[\text{Pb}_7(\text{OH})_3\text{F}(\text{BO}_3)_2(\text{CO}_3)] [\text{Mg}_{4.5}(\text{OH})_3(\text{Si}_5\text{O}_{14})]$ ,  $P1$

Chalcodite,  $\text{K}(\text{Fe}^{3+}, \text{Mg}, \text{Fe}^{2+})_8(\text{Si}, \text{Al})_{12}(\text{O}, \text{OH})_{27}$ ,  $P1$

Cookeite,  $\text{LiAl}_4(\text{Si}_3\text{Al})\text{O}_{10}(\text{OH})_8$ ,  $C2$  (or  $Cc$ )

Cymrite,  $\text{BaAl}_2\text{Si}_2(\text{O}, \text{OH})_8 \cdot \text{H}_2\text{O}$ ,  $P2_1$

Dmisteinbergite,  $\text{Ca}(\text{Al}_2\text{Si}_2\text{O}_8)$ ,  $P312$

Ekanite,  $\text{Ca}_2\text{ThSi}_8\text{O}_{20}$ ,  $I422$  (the only chiral mineral in that space group, Table 3)

Kaolinite,  $\text{Al}_2\text{Si}_2\text{O}_5(\text{OH})_4$ ,  $P1$

Latiumite,  $(\text{Ca}, \text{K})_4(\text{Si}, \text{Al})_5\text{O}_{11}(\text{SO}_4, \text{CO}_3)$ ,  $P2_1$

Levantite,  $\text{KCa}_3\text{Al}_2(\text{SiO}_4)(\text{Si}_2\text{O}_7)(\text{PO}_4)$ ,  $P2_1$

Searlesite,  $\text{NaBSi}_2\text{O}_5(\text{OH})_2$ ,  $P2_1$

Zussmanite,  $\text{K}(\text{Fe}, \text{Mg}, \text{Mn})_{13}(\text{Si}, \text{Al})_{18}\text{O}_{42}(\text{OH})_{14}$ ,  $R3$

### 4.3.2. Opals

Yet another interesting silica polymerization/precipitation/crystallization process, is the formation of *opal*,  $\text{SiO}_2 \cdot n\text{H}_2\text{O}$ , a hydrated amorphous/microcrystalline mineraloid. It is formed by solution polymerization of monomeric and oligomeric silicic acid into amorphous silica, which, upon slow evaporation precipitates as layers of spheres, 150-350 nm in size. These may give rise to the beautiful diffractive coloration and fluorescence utilized by the gemstone industry. The amorphous phase co-exists with slowly forming silica crystalline phases – interestingly, the chiral ones - which has led to classification of various opals: opal-C, which contains well-ordered  $\alpha$ -cristobalite, opal-CT (lussatine, lussatite) which contains disordered clusters of  $\alpha$ -cristobalite and  $\alpha$ -tridymite, (and opal-A, which is highly disordered and nearly fully amorphous). Opal is therefore an example polymorphic changes which take place in solution. Despite the fact that natural opals contain the chiral crystalline silica polymorphs of cristobalite and tridymite, opal is not chiral on a macroscopic level because these crystals appear there as conglomerate mixtures; short range order may reveal specific handedness, but again, I am not aware of attempts to detect it.

#### 4.3.3. Ambers

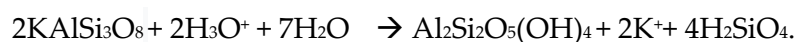
Ambers consist of a family of fossilized chiral polymeric, non-crystalline bioorganic resins of the approximate empirical formula of  $C_{12}H_{20}O$ , representing a mixture of bioorganic components. In Dana and Strunz classifications amber is considered an organic mineral, but not so by IMA (since they formed biochemically), but they do appear in most mineral listing – mindat lists as many as 19 different ambers (Amber, <https://www.mindat.org/min-188.html>). Ambers are chiral because they are composed mainly of polymerized and oligomerized diterpenoids such as the labdanoids (note that we already encountered the diterpenoids as the most common source of chiral organic minerals – Section 3). These chiral building blocks polymerize to various degrees and to various compositions, resulting in a chiral mixture of polymeric phases, oligomers and monomers (Armstrong et al, 1996). The biological origin of ambers renders their handedness to be of a single enantiomorph (for instance the handedness of the labdan main building block is (4aR,5S,6S,8aS)-1,1,4a,6-tetramethyl-5-[(3R)-3-methylpentyl]decahydronaphthalene).

#### 4.4. Chemical Transformations of Chiral Minerals

Another major route of the natural synthesis of minerals, is the chemically reactive transformation of existing minerals, usually primary minerals into secondary minerals. Such transformations are intimately linked to the useful concept of minerals evolution (Hazen and Morrison, 2022). Common mineral transforming chemical reactions are hydrolyses, oxidations, weathering reactions with  $CO_2$ , and ion-exchange reactions. Here are few representative examples, which involve the formation of, or reaction with, chiral minerals:

##### 4.4.1. Hydrolyses

In the previous section we saw mineral changes and chirality alterations due to hydration or dehydration of minerals, in which water molecules are usually ligands of metal cations. We now continue with hydrothermal processes which involve changes in covalent bonds. Perhaps the widest class of hydrolytic reactions is serpentinization. In this class of reactions, minerals - mainly silicates (such as olivines ( $(Mg,Fe)_2SiO_4$ ) and pyroxenes ( $(Mg,Fe)SiO_3$ )) - are hydrolyzed into hydroxyl-rich silicates – serpentines. Serpentinization is capable of inducing chirality in the hydrolyzed product, and examples of chiral serpentines include amesite,  $Mg_2Al(AlSiO_5)(OH)_4$ , P1; kellyite,  $Mn^{2+}_2Al(AlSiO_5)(OH)_4$ , P6<sub>3</sub>; and the 2H2 polytype of guidottiite,  $Mn_2Fe^{3+}(Fe^{3+}SiO_5)(OH)_4$ , P6<sub>3</sub>. Serpentinization reaction mechanisms are often represented by an overall reaction equation, which summarizes a complex multistep process, and a typical example is the serpentinization of orthoclase, the K-feldspar  $KAlSi_3O_8$  which is an achiral tectosilicate (C2/m), into kaolinite (chiral, P1), which belongs to the larger kaolinite-serpentine group):



As shown in this reaction, hydrolyses are also often accompanied by ion-exchanges, which contribute too to the chemical transformation of the mineral. In our example,  $Al^{3+}$  replaces  $K^+$  and the  $Si_3O_8^{4-}$  unit is cleaved-hydrolyzed to two shorter Si units. More on the silicate component transformation, in the next family of reactions (carbonations). Finally, note that the serpentinization of an achiral mineral which results in a chiral mineral, in fact produces two different minerals – the left-handed enantiomorph, and the right-handed one – usually at a 1:1 proportion. The same is true for the next mineral reactions, and in fact for any conversion of an achiral mineral to a chiral product.

##### 4.4.2. Carbonations

Reactions of minerals with  $CO_2$  have attracted much recent attention in the context of its atmospheric sequestration by capturing it with silicates, especially  $Ca^{+2}$  and  $Mg^{+2}$  silicates (Daval, 2018) and with carbonates (Pogge von Strandmann et al, 2019). Carbonations belong also to the class of hydrolytic reactions, because the actual reactive species – the bicarbonate and the carbonate anions, which are obtained by the hydrolysis of dissolved  $CO_2$  in water:



In our context, here is an example for the loss of chirality due to a carbonation reaction – the conversion of combeite,  $\text{Na}_2\text{Ca}_2\text{Si}_3\text{O}_9$  (P3<sub>1</sub>21/P3<sub>2</sub>21), into calcite and silica, driven by the precipitation of these sparingly soluble products:

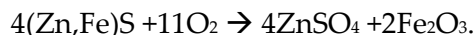


Some further comments are due on this example: First, note that the direction of erasing chirality, means a conversion of a conglomerate of two enantiomorphous  $\text{Si}_3\text{O}_9^{4-}$  skeletons into a single achiral mineral – amorphous  $\text{SiO}_2$  (Kremer et al, 2022). Second, the correct way to report the silica formation in the reaction equation, is not the traditional accepted way -  $\text{SiO}_2$  – which appears in the carbonation literature and reproduced above, but as the polymeric  $(\text{Si}_3\text{O}_9^{4-})_n$ . These anions as well as their silanols (obtained through  $-\text{SiO}^- + \text{H}_2\text{O} \rightarrow -\text{SiOH} + \text{OH}^-$ ), condense into the siloxane units,  $-\text{SiOSi}-$ , catalyzed by the released  $\text{OH}^-$ , forming amorphous silica.

#### 4.4.3. Oxygenations

Oxygenations are particularly interesting and important because of the massive increase in the high oxidation-number minerals following the Great Oxygenation event (Hummer et al, 2022), and because Earth atmosphere is still highly oxidative. Oxidations may erase chirality or preserve that property in their products – let us focus in this section on oxidative formation of chiral minerals. Chiral minerals of metal cations at their higher oxidation states, may have started their paragenetic geologic journey in their metallic form or as cations of low oxidation states. For instance, the chiral Mn minerals, ernienickelite,  $\text{NiMn}^{4+}_3\text{O}_7 \cdot 3\text{H}_2\text{O}$  and urorite  $\text{Mn}^{2+}\text{Mn}^{4+}_3\text{O}_7 \cdot 3\text{H}_2\text{O}$ , both of space group R3, could be the oxidation products of earlier  $\text{Mn}^{+2}$  minerals (Hummer et al, 2022). Likewise, the chiral uranium mineral, wyartite,  $\text{CaU}^{5+}(\text{U}^{6+}\text{O}_2)_2(\text{CO}_3)\text{O}_4(\text{OH}) \cdot 7\text{H}_2\text{O}$ , P2<sub>1</sub>2<sub>1</sub>2<sub>1</sub>, is probably an oxygenation product of earlier  $\text{U}^{4+}$  minerals (Hazen et al, 2009).

Metallic minerals where the metal is in its native zero-valency form are prone to oxidations, particularly if they are not of the noble-metal family. An interesting example in our context is the chiral metal-alloy moschellandsbergite,  $\text{Ag}_2\text{Hg}_3$ , space-group I23, which is a potential source for Ag and Hg cations, potentially finding their way to chiral minerals such manganosquarite,  $\text{AgMnAsS}_3$ , P4<sub>1</sub>22/P4<sub>3</sub>22, schuetteite,  $\text{Hg}_3(\text{SO}_4)\text{O}_2$ , P3<sub>1</sub>21/P3<sub>2</sub>21, and more. As for the non-metal elements in minerals, these too may appear in various oxidation states. Sulfur minerals, for instance, can be found in all of its oxidation states, from -2 to +6, and in fact, one of the more important geological oxidations is from the sulfide (-2) all the way up to the sulfate (+6). For instance, this extreme oxidative transformation is attributed to the formation of the chiral goslarite,  $\text{ZnSO}_4 \cdot 7\text{H}_2\text{O}$  (P2<sub>1</sub>2<sub>1</sub>2<sub>1</sub>) from the achiral sphalerite  $(\text{Zn},\text{Fe})\text{S}$ , (Goslarite Mineral Data, <https://webmineral.com/data/Goslarite.shtml>):



Regarding the chiral elemental non-metal mineral selenium and the elemental metalloid mineral tellurium, both described above, their cations appear too in minerals in various oxidation states, and chiral minerals of higher oxidation states, which may have started their oxidative routes from the element, are documented, including the chiral minerals chalcomenite,  $\text{Cu}(\text{Se}^{4+}\text{O}_3) \cdot 2\text{H}_2\text{O}$ , P2<sub>1</sub>2<sub>1</sub>2<sub>1</sub>, fairbankite,  $\text{Pb}^{2+}_{12}(\text{Te}^{4+}\text{O}_3)_{11}(\text{SO}_4)$ , P1, and even the extreme +6 oxidation state in leisingite,  $\text{Cu}_2\text{MgTe}^{6+}\text{O}_6 \cdot 6\text{H}_2\text{O}$ , P3.

## 5. Chirality of the Macroscopic Mineral

### 5.1. Molecular Level Descriptors of the Macroscopic Crystal

#### 5.1.1. The Crystal Class

The outcome of the various mineral formation routes described in Section 4, is the macroscopic mineral, from the microns to cm and even to meter scales. The molecular level should lead to some

predicted ideal macroscopic shape, but in reality, the actual final shape – the habit – of the grown mineral, may have little resemblance, if at all, to that ideal shape. Nevertheless, in this Section and in the next Section 5.1.2, we briefly describe the idealized expectation, before moving to the real, found-in-field, shapes.

The combined collection of all molecular building blocks of a crystal, namely the molecular array of the whole crystal, has a symmetry of its own. That macroscopic symmetry carries with it the symmetry characteristics of the molecular assembly in the elementary UC, but without the translational glide elements (because translating the whole crystal is just shifting it to a different place); we are therefore back in the domain of point-group symmetries for the description of the macroscopic symmetrical shape. The crystallographic restriction of having symmetrical 3D space filling arrays, limits the number of possible whole crystal point-group symmetries to 32 ( $31+C_1$ ). These are called the **32 crystal classes** or **crystallographic point groups**, and each is labeled by its Hermann-Maguin (HM) or Schoenflies (Sch) point group notations (Hahn and Klapper, 2006). Crystal classes appear routinely in listings of minerals as one of their main characteristics, also because they are linked to a variety of chemical and their physical characteristics (Section 6). 11 of the 32 crystallographic point groups contain only rotational elements – see Table 1, first column – and describe the only 11 possible whole-crystal molecular assembly symmetries of chiral crystals. It is also seen in that table why these are termed “Classes”: Each class contains all space-group symmetries which share the same collection of rotational symmetry elements (roto-glide elements are treated with their rotational part only, without the gliding operation). For instance, the chiral 222-crystal class ( $D_2$  point-group symmetry) encompasses all space groups which have three perpendicular 2 ( $C_2$ ) rotational axes, including the axis of the  $2_1$  roto-glide. As this class is composed of rotational elements only, it describes, by definition, only chiral crystals. We have now therefore third version for a common chiral mineral identifier:

---

**A mineral is chiral only if its crystal class contains only rotational elements, including the identity**

---

In addition to the symmetry point group label of the crystal class, the macroscopic crystal is also traditionally described by an ideal shape – *open* or *closed* - which has that point-group symmetry – see Table 1, first column: An example for an open shape there is the 2 ( $C_2$ ) sphenoid – two faces related by a  $C_2$  rotational symmetry; and an example for a closed shape is the 222 ( $D_2$ ) rhombic-disphenoidal polyhedron, which is a tetrahedron with all faces being scalene triangles, rendering it chiral (Disphenoid, <https://en.wikipedia.org/wiki/Disphenoid>). This polyhedron as well as all other shapes associated with 11 chiral classes, appear as left – and right-handed versions (see (External Symmetry of Crystals, 32 Crystal Classes, <https://www2.tulane.edu/~sanelson/eens211/32crystalclass.htm>) for the shapes of all chiral crystal classes).

To put this classification in relevance, we already mentioned in this review quite a number of minerals which belong to the 222 crystal class, most of which are in the common space group  $P2_12_12_1$ , namely nabesite ( $\text{Na}_2\text{BeSi}_4\text{O}_{10} \cdot 4\text{H}_2\text{O}$ ), epsomite, goslarite, and morenosite ( $\text{MSO}_4 \cdot 7\text{H}_2\text{O}$ , where  $M = \text{Mg}, \text{Zn}, \text{Ni}$ , respectively), wyartite ( $\text{CaU}^{5+}(\text{UO}_2)_2(\text{CO}_3)\text{O}_4(\text{OH}) \cdot 7\text{H}_2\text{O}$ ), chalcomenite ( $\text{Cu}(\text{Se}^{4+}\text{O}_3) \cdot 2\text{H}_2\text{O}$ ), austinite ( $\text{CaZnAsO}_4(\text{OH})$ ), leucophanite ( $\text{NaCaBeSi}_2\text{O}_6\text{F}$ ), umbite ( $\text{K}_2(\text{Zr,Ti})\text{Si}_3\text{O}_9 \cdot \text{H}_2\text{O}$ , and leucophanite ( $(\text{Na,Ca})_2\text{BeSi}_2(\text{O.OH.F})_7$ ). We have already mentioned also minerals with other space groups belonging to the 222 class: tridymite ( $\text{SiO}_2$ ,  $C222_1$ ), edingtonite ( $\text{Ba}(\text{Al}_2\text{Si}_3\text{O}_{10}) \cdot 4\text{H}_2\text{O}$ ,  $P2_12_12_1$ ), gismondine-Sr ( $\text{Sr}_4(\text{Si}_8\text{Al}_8\text{O}_{32}) \cdot 9\text{H}_2\text{O}$ ,  $C222_1$ ), and tobermorite ( $\text{Ca}_5\text{Si}_6\text{O}_{16}(\text{OH})_2 \cdot 4\text{H}_2\text{O}$   $C222_1$  (or  $P2_1$ )).

The 32 crystal classes are traditionally divided into 7 **crystal systems**. While these do not provide information on the chirality/achirality of a crystal, we briefly describe it here, as this classification appears in most mineral listings. A crystal system groups the crystal classes (and the space groups they contain) that utilize the same lattice system. Thus, it divides the 32 crystal classes between, the cubic, hexagonal, trigonal, tetragonal, orthorhombic, **monoclinic**, and the **triclinic** lattices <sup>Note 9</sup>. For instance, the tetragonal crystal system groups seven crystal classes (out of the 32), two of which are



chiral and appear in Table 1 (first column): The 4 ( $C_4$ , tetragonal-pyramidal) and 422 ( $D_4$ , tetragonal-trapezohedral) crystal classes; see Table 1 first column for the other crystal system-crystal class relations.

### 5.1.2. The Crystal Forms

Next, we explain the how the crystal classes just described, give rise to many possible macroscopic crystal forms. For that we first recall that the habit is often characterized by clearly observed planar faces. These faces indicate where the crystal develops grows, and where possible cleavage planes of the crystal exist, which are parallel to those external faces. The mutual orientations of these faces on the macroscopic habit are dictated by the symmetry and geometrical arrangement details of the atoms – specifically by their symmetry class - and by the lattice which packs them. These planes are termed *crystallographic faces* (or planes, which are defined by their *Miller index* labels <sup>Note 10</sup>. Out of the various possible growth/cleavage planes, one may build a variety of geometrical bodies, which are termed *crystal forms*. Crystallography considerations lead to of 47 (Hahn et al, 2016) or 48 (Perkins et al, 2023) possible crystal forms (depending on the methodology), the faces of which are those of the crystal classes. A given crystal class is associated in most cases with more than one crystal form, resulting in either achiral or chiral forms. For instance, the 222 ( $D_2$ ) crystal class may give rise to crystal forms such pinacoid, rhombic disphenoid, and rhombic prism (Hahn and Klapper, 2006.). The opposite is also true: A specific crystal form may result from several different crystal classes. For instance, the tetragonal prism crystal form may emerge from the chiral 4 and 422 classes and from a number of achiral classes (4/m and more). For a full table of all general crystal forms and the specific classes, chiral and achiral that are associated with them, see (Perkins et al, 2023).

In reality crystals the situation is much richer from the shapes point of view, because crystals often grow (or are cleaved) along faces which come from a combination of several forms which are allowed by a specific crystal class. From that point of view, the term "crystal form" is somewhat misleading, and one should therefore regard the "crystal form" as a "form-unit building block". A nice example is quartz, which is found in nature with as many as 40 different combinations of the crystal forms which belong to its crystal class 32 ( $D_3$ ), some chiral, others achiral, including the most commonly cited chiral habit of quartz, which is in fact a combination of 5 crystal forms, preserving macroscopically the 32 symmetry classes – see (The Quartz Page, [http://www.quartzpage.de/crs\\_forms.html](http://www.quartzpage.de/crs_forms.html)) for details. The same is true for achiral minerals, an example being calcite,  $\text{CaCO}_3$ , which may occur in either achiral or chiral (scalenohehdral) forms (Hazen, 2004).

## 5.2. Chiral Habits of Minerals

### 5.2.1. Growth Conditions and Randomness as Sources of Habit Chirality

The combinations of crystal forms described in the previous section are not the sole contributors to the actual final crystal habit, either as a large single crystal, or of the individual crystallites in aggregates. The faces of the combinations of crystal forms are the growth-process playgrounds, and the rates of growth of the various faces are affected by a host environmental processes and parameters which can also switch off a given face altogether. One of the main affecting parameters are specific ions or (bio)molecules in relatively small concentrations, which have different adsorption affinities to the various crystal faces (Addadi and Geva, 2003). These diverse environmental parameters may result in either chiral or achiral habits, and quite often, *with no connection to the chirality/achirality* as dictated by the space-group and the crystal class. It is for that reason that the symmetry/chirality descriptors of minerals use mainly the space-group and the symmetry class, with the understanding that resulting shape of the habit is not uniquely defined. Indeed, the variety of habit shapes is practically endless, but it is still customary to use broadly defined shape-adjectives such as pyramids, cubes, tetrahedra, dipyramids, etc. However, one should bear in mind that actual habits are rarely of these ideal shape descriptors – distortions, fractures, defects, weathering processes, co-crystallization

of more than one mineral, disappearance of faces, variations during the history of formation - all lead to habits which in most cases only roughly are ideally shaped.

In particular, bear in mind that practically all of the parameters that affect the mineral growth, always have some elements of randomness in them – they are fluctuating, non-homogeneously distributed, and occur in non-isotropic environments. *Randomness is therefore a source of uniqueness for each mineral species and a source of external shape chirality.* In other words, the majority minerals in their as-found condition are of shape that is unique for that find – the chances of finding an exact duplicate in size, and shape, and location and distribution of defects, is practically zero. This is clearly evident for habits which are of clustered and aggregated shapes - radial needles, botryoidal cluster (a cluster of rounded spheroidal shapes), fibrous clusters, dendrites, etc., but is true also for minerals which preserve a near polyhedral shape. That being the case, we reach another, perhaps unexpected conclusion: *When it comes to habits, most minerals are chiral:* The chance of preserving an exact mirror symmetry during growth or degradation processes of the mineral is very low. In other words, *randomness leads to chirality*, which is termed **incidental chirality** (Katzenelson et al, 1996). And it is a special kind of chirality, because by the same token, that external chirality is single enantiomorphic – the probability of finding an exact counter-enantiomorph by processes which include an element of randomness (that is, an exact mirror image enantiomorph), is practically zero. At most, one can speak in this case about “near-enantiomorphs” (Katzenelson et al, 1996). Given the fact that the specific habit is so sensitive to growth conditions, how is it that the two near-enantiomorphic crystal habits can still be identified as such by visual inspection? This is so because the environment in which the two enantiomorphs have grown has no handedness bias, and therefore preserve some degree of mirror-reflection similarity between left-handed growth and a right-handed growth (up to the effects of randomness).

It is in order to comment here that dendritic minerals, such as the well-known dendritic precipitation growth of a variety of MnO<sub>2</sub> inside calcite and other minerals, have scale-invariance symmetry, also known as a fractal shape symmetry (Avnir, 1989), and again, not two dendrites are the same, and all are chiral, without having exact two enantiomorphic shapes – only near-enantiomorphs are possible.

### 5.2.2. Chiral Twins

The phenomenon of twinning relates to cases where two (or more) crystals of a mineral are fused together into a semi-symmetrical joint habit. The fusing occurs through one of the crystallographic planes either as a contact plane or as an inter-penetration zone through that plane. In Section 3 we have seen cases (cyrilovite, leucophanite), where the two enantiomorphs of chiral crystals were identified in twinned structures. Well-known are the twinning arrangements (termed “laws”) of quartz the most common of which are the Brazil-law twins and the Dauphiné-law twins. In fact, it is generally accepted that twinned quartz by these two laws is more common than un-twinned quartz (Gault, 1949). In Brazil twins the two opposing enantiomorphs are fused together, while in Dauphiné twins the fusing is of either right-handed or left-handed enantiomorphs. Thus, in Dauphiné twins, the whole twinned crystal is always molecularly and macroscopically chiral, either left-handed or right-handed. This not the case for Brazil twins which may be either achiral or chiral as a whole: They are achiral if the two enantiomorphic sections are aligned through a symmetry plane, reflecting one enantiomorph into the other (the “twin plane”), or through inversion symmetry (“inversion twins”, “twin center”). Any other alignment of the components results in a Brazil twin, results in a chiral overall shape (very much as we have seen for kryptoracemates (Section 2.7)) <sup>Note 11</sup>. It should also be noted that combined twinning - Dauphiné-Brazil – exists as well (Gault, 1949).

### 5.2.3. Chiral Habits of Biominerals

Living organisms synthesize, precipitate and use minerals to build a wide variety of structured biomaterials, a phenomenon known as **biomineralization**. Most minerals in that category are carbonates (calcite or aragonite), phosphates and amorphous silica. Continuing the theme of the role of randomness in dictating chirality (Section 5.2.1), there are two types when it comes to biological

formation of the skeletal minerals. The first follows the randomness argument detailed above, leading to precipitated biomaterials the chirality of which is purely incidental. The second type is more complex and involves the active participation of biomolecules and biopolymers in the building process of the mineral. The involvement of these natural morphology directing agents dictates biomaterial chiral habits which in many cases are of single enantiomorph. Many chiral structures fall into that category and a classical example are the helical calcium carbonate structures of mollusk shells, usually of a single enantiomorph per species. Likewise, one can find chirally-shaped calcium carbonate skeletons of foraminifera and coccolithophore.

Interestingly, the chiral biomolecules used as templates in these biological growth processes, can induce chiral habits even in crystals which are of improper-elements space groups (Bouropoulos et al, 2001). For instance, gypsum,  $\text{CaSO}_4 \cdot 2\text{H}_2\text{O}$ , is achiral (of space group  $I2/a$ ) but growing it in the presence of L-lysine, results in a chiral crystal habit (Cody and Cody, 1991). Yet another example is the induction of chiral habits in vaterite, the achiral  $\mu$ -polymorph of  $\text{CaCO}_3$ , which is of space group  $P6_3/mmc$ , by the use of the enantiomers of asparagine (Jiang et al, 2019). In many instances – coccoliths, for instance - the exoskeleton of which is calcite, has plenty of forms, some of which are chiral and of single enantiomorph (Avrahami et al, 2022).

### 5.3. Chiral Gemstone Minerals

An important aspect of the macroscopic appearance of minerals, is their utilizations as gemstones. Minerals which are used in the gem industry utilize either chemically pure crystals, but more often crystals which are doped with characteristic impurities, rendering their effect as typical color, lust, luminescence, and other aesthetic features which are enhanced in the final product. Ion impurities maybe incorporated in the crystal lattice replacing the original atoms (Götze et al., 2021), while larger species are entrapped in crystal dislocations or co-precipitated. These processes occur either during the crystal formation or in later processes such as under hydrothermal alterations (Liu et al, 2023). Particularly large raw gemstone minerals are found in pegmatites igneous rocks, which crystallize from concentrated solutions that separate from a magma in small pockets; an example of a pegmatite chiral mineral used as a gemstone is the phosphate cyrilovite already, mentioned above (Cyrilovite, <https://gemstone.fandom.com/wiki/Cyrilovite>).

Generally, inclusion of impurities in chiral minerals do not change their space-group symmetry, and chirality is retained. Chiral gems therefore should appear as left- or right-handed enantiomorphs, and *I am unaware of commercial utilization in the gem industry of that distinction*. It should be noted however that as this enantiomorphism refers to the molecular level chirality of the gems – the artificial macroscopic cutting shape may be either chiral as well, or achiral.

From listings of minerals suitable or already used as gemstones (List of gemstones by species, [https://en.wikipedia.org/wiki/List\\_of\\_gemstones\\_by\\_species](https://en.wikipedia.org/wiki/List_of_gemstones_by_species) and other listings), here is a collection of chiral minerals that give rise to the option of having left- and right-handed molecular level gem versions (some have been already mentioned):

#### List of chiral gemstones

Austinite,  $\text{CaZnAsO}_4(\text{OH})$ ,  $P2_12_12_1$   
 Cancrinite,  $\text{Na}_6\text{Ca}_2[(\text{CO}_3)_2\text{Al}_6\text{Si}_6\text{O}_{24}] \cdot 2\text{H}_2\text{O}$ ,  $P6_3$   
 Celadonite,  $\text{K}(\text{Mg}, \text{Fe}^{2+})(\text{Fe}^{3+}, \text{Al})[\text{Si}_4\text{O}_{10}](\text{OH})_2$ ,  $C2$   
 Cinnabar,  $\text{HgS}$ ,  $P3_12_1$  and  $P3_22_1$   
 Cyrilovite,  $(\text{NaFe}^{3+}_3(\text{PO}_4)_2(\text{OH})_4 \cdot 2(\text{H}_2\text{O}))$ ,  $P4_12_12/P4_32_12$   
 Ekanite,  $(\text{Ca}, \text{Fe}, \text{Pb})_2(\text{Th}, \text{U})\text{Si}_8\text{O}_{20}$ ,  $I422$   
 Kaolinite,  $\text{Al}_2\text{Si}_2\text{O}_5(\text{OH})_4$ ,  $P1$   
 Langbeinite,  $\text{K}_2\text{Mg}_2(\text{SO}_4)_3$ ,  $P2_13$   
 Leucophanite,  $(\text{Na}, \text{Ca})_2\text{BeSi}_2(\text{O}, \text{OH}, \text{F})_7$ ,  $P2_12_12_1$   
 Nepheline,  $\text{Na}_3\text{KAl}_4\text{Si}_4\text{O}_{16}$ ,  $P6_3$   
 Quartz-based gemstones – see below  
 Searlesite,  $\text{NaBSi}_2\text{O}_5(\text{OH})_2$ ,  $P2_1$   
 Simpsonite,  $\text{Al}_4(\text{Ta}, \text{Nb})_3\text{O}_{13}(\text{OH})$ ,  $P3$

Thaumasite,  $\text{Ca}_3\text{Si}(\text{OH})_6(\text{CO}_3)(\text{SO}_4) \cdot 12\text{H}_2\text{O}$ ,  $P6_3$

Vishnevite,  $(\text{Na}, \text{Ca}, \text{K})_6(\text{Si}, \text{Al})_{12}\text{O}_{24}[(\text{SO}_4), (\text{CO}_3), \text{Cl}_2]_{2-4} \cdot n\text{H}_2\text{O}$ ,  $P6_3$

Wardite,  $\text{NaAl}_3(\text{PO}_4)_2(\text{OH})_4 \cdot 2(\text{H}_2\text{O})$ ,  $P4_12_12/P4_32_12$

Weloganite,  $\text{Na}_2(\text{Sr}, \text{Ca})_3\text{Zr}(\text{CO}_3)_6 \cdot 3\text{H}_2\text{O}$ ,  $P1$

As a family of gemstones, quartz is a rich source in general, and by far the richest source of chiral gemstones, all of which are basically  $\text{SiO}_2$  at  $P3_121/P3_221$  space-groups. Examples include: Amethyst, aventurine, chalcedony microcrystalline stones (such as agate, carnelian, chert, chrysoprase, heliotrope, onyx, pietersite and sard), citrine, dumortierite quartz, pink quartz, prase, prasiolite, milky quartz, rose quartz, smoky quartz (morion), tiger's eye and hawk's eye, mixed gemstones such as ametrine (trystine, bolivianite), opal, and more at (The Mineral Quartz, <https://www.minerals.net/mineral/quartz.aspx;%20https://www.mindat.org/min-3337.html>). Jewelry is prepared also from microcrystalline quartz minerals – jasper, carnelian, chalcedony, onyx, agate, chert, and flint – all of which are most probably a conglomerate of 1:1 of the two enantiomorphs of quartz. Many of the specific colors are attributed to the effect of natural irradiation, which produce the entrapped metal-cation-colored ionized centers. For instance, smoky quartz probably gets its color by irradiation of aluminum impurities within the crystalline quartz, amethyst typical purple color is the result of irradiation triggered electron shuttling between  $\text{Fe}^{3+}$  and  $\text{Fe}^{4+}$ , and so on. More on minerals coloration can be found in the classical review of Nassau (Nassau, 1978).

A major aspect of this industry is the cutting and polishing into a wide library of shapes, mainly polyhedral. Artificial chiral cuts (artificial chiral habits) do exist, such as the Dreamscape™ Cut (Ruby Dreamscape™ Cut, <https://www.johndyergems.com/gemstones/ruby-7397.html>). I am unaware of a recognition that such cuts may be made as either a left-handed or a right-handed polymorph; it matters because the aesthetic perception of left or right objects, is different (Avnir and Huylebrouck, 2013).

#### 5.4. Handedness Labeling of the Chiral Minerals

##### 5.4.1. The Problem of Handedness Labeling

Once we have established that we have a chiral mineral species at hand, how should we label its handedness? Is it the left-handed mineral or a right-handed one? While connected, the concepts of chirality and handedness are inherently different terms: Chirality is a structural property, which is manifested by the appearance of two mirror-imaged enantiomorphs which cannot be superimposed. Handedness, on the other hand, is not a structural property but an arbitrary, agreed label to help us distinguish between the two enantiomorphs. For instance, we can decide that from now we switch the left-right labeling method of helices – the chirality of what was labeled as left remains unchanged, we just call it now “right”.

Having that distinction in mind, the question of handedness assignment is further confused by the fact that the space-group, the various possible fragments of the molecular building blocks of the mineral, and the macroscopic habit, do not necessarily carry all the same handedness label (all “left” or all “right”), but are often mixed. For instance, the quartz enantiomorphic habit which is labeled as left-handed has the space-group symmetry of  $P3_121$ , that is, a right-handed helical glide component, a structural sixfold Si-O-Si helix turning counter-clockwise (left), a structural threefold helix which turns clockwise (right) (The Quartz Page, <http://www.quartzpage.de/>), and optical rotation to the left (Van Dyke, 1940). This confusing situation of quartz, was reviewed by Glazer (Glazer, 2018), and is, in fact common to most chiral minerals. True, the simplest recognition that one has at hand a chiral mineral with two enantiomorphic versions is seeing it with the naked eye or under a microscope – that is, Pasteur-type recognition that there are two habits, which are mirror images of each other. Handedness rules for habits have been formulated – see their implementation for quartz enantiomorphs (Van Dyke, 1940) – however, it has been of limited general applicability, because in the majority of cases, the actual habit of chiral minerals blurs the existence of two enantiomorphs. The molecular structure, however, is free of that habit problem, because it remains unchanged, regardless of the actual habit.



The next choice to make then is what fraction of molecular structure of the crystal should be taken for the handedness labeling, once the absolute configuration has been determined? The content of the UC with its space-group symmetry? a molecular fragment within the UC? and which one? Trying to generalize convention-rules for the entire domain of chiral minerals is not an easy task because of the endless possibilities of structures fulfilling the definition of chirality. Therefore, the approach we adopt is to offer a short list of options, each tailored for specific large family of chiral minerals.

We begin with the minerals in the 22 enantiomorphic space groups. Here, once the absolute configuration was determined, the simplest way to label the handedness is to look at space group description of the UC, and specifically at the roto-glide element of the space group. Thus, a chiral mineral in space group  $P4_1$  (for instance percleveite-(La) $_{-}$ La $_2$ Si $_2$ O) will be labeled as a right-handed mineral, while the same mineral will be left-handed, if found at  $P4_3$ .

As already mentioned above, the main problem is linked to the remaining 43 non-enantiomorphic Söhncke space groups – here the space-groups methodology, does not provide a distinction between the two enantiomorphs. A general set of rules to distinguish between left-handed and right-handed molecular arrangements of the UC, do not yet exist. Detailed convention rules were developed - mainly for organic and organometallic molecules – and these are the IUPAC official R/S (right/left) Cahn-Ingold-Prelog (CIP) convention, the classical D/L (right/left) convention, and the helical delta/lambda (right/left) and P/M (right/left) conventions. Because of that arbitrariness of the agreed conventions, it could well be that a specific chiral object which is labeled left-handed by one convention is labeled right-handed by another one (an example being the “left-handed” amino acid L-cysteine which flips to become “right” handed under the R/S convention (Avnir, D., 2021)). In fact, it has been shown that for any set of handedness-assignment rules, one can find chiral structures for which it is not possible to say if the structure is left- or right-handed (termed “non-handed” (Pinto et al, 1996) or “latent” chirality (Pinto and Avnir, 2001)). If the UC is composed of one chiral molecule (in a non-bisected way), that is, the number, Z, of the formula units is 1, then these rules can be applied, and the handedness of the mineral will be labeled as the handedness of that one molecule within the UC (and the same is true for higher Z values of chiral molecules within the UC). Yet another option for labeling the handedness of minerals in the 43 non-enantiomorphic crystals, is to isolate from the molecular structure, a characteristic sub-unit which carries the chirality. For instance, as mentioned in Section 2.6, many minerals carry the common the  $T(-O-T')_4$  unit, where T and T' are, e.g., Si, Al, Be, etc. In these cases, it is useful to determine the handedness of the  $TT'_4$  distorted tetrahedron (that is, the  $T(-O-T')_4$  unit without the oxygens), by the method for labeling the handedness of general tetrahedral  $AB_4$  structures, described in detail in (Yogev-Einot and Avnir, 2004; Dryzun et al, 2009).

And yet, in many cases, the existing conventions are not always applied easily, if at all, to the specific case of the UCs of minerals. It is the arbitrariness of the handedness conventions that points to a possible practice in such cases, and that is that the report attaches the handedness way in an arbitrary way, provided that the images of the left and right UC structure of the left and right habits are shown with their specific handedness assignments (for instance, L-P212121 and R-P212121). We have already seen in Section 3 that this, indeed has been the practice, already in several reports.

### 5.4.2. The Enantiomeric Excess

The expected outcome of the synthesis or transformation of chiral minerals by any of the previously described routes, is a conglomerate of 1:1 ration of the two enantiomorphs; that is, at a location where such minerals are found, both enantiomorphs should be there at approximately that ratio. This is so, because most natural environments where minerals form, do not have enantiomorphic components by themselves (an exception are the biominerals). While an ideal conglomerate has an exact 1:1 ratio of the two enantiomorphs, in practice that ratio may be only close to it. For instance, if the chiral mineral is of sand small particles morphology (quartz sand, for instance), then the ratio should be quite close to 1:1, but at a location of few large crystals, that ratio need not be of that value. The extreme situation of forming *all* of the crystals with an identical handedness – **homochiral crystals** – is well documented in synthetic laboratory chemistry and there are several mechanisms leading to it, such as the Viedma mechanism (Iggland and Mazzotti, 2011), which is an Ostwald-ripening type of process, but I am unaware of a similar report in mineralogy (except of course for the rare event that just one good crystal of the chiral mineral is found on site).

In between the two extremes – from a 1:1 conglomerate to 1:0 homochiral crystals - the whole range of enantiomorph ratios is in principle possible; such mixtures are termed **scalemic** mixtures. That ratio is termed the **enantiomorphic excess** (ee) for crystals, and **enantiomeric excess** for molecules, and it is expressed as

$$ee \equiv A - B$$

where A,B are the mole or weight fractions, of the major and minor enantiomorphs/enantiomers in that order (regardless of their handedness labeling), so that  $A+B = 1$ . Exact conglomerates have an ee of  $0.5 - 0.5 = 0$ , and pure enantiomorphs (homochiral crystals) have an ee of  $1.0 - 0.0 = 1.0$ . The enantiomeric excess is also commonly presented as  $ee\% = (A-B)100$  or as  $100(A'-B')/(A'+B')$  where  $A',B'$  are in moles. Alternatively, the absolute value of  $(A-B)$  is taken, regardless of which of the two is the major component - all of these expressions are equivalent. A main case of ee determination has been that of quartz, where small local excesses have been observed (Támara and Preston, 2009). These maybe attributed to fluctuation in the crystallization process, to impurities of bio-organic origin, and more (we return to it in Section 6.4).

## 6. Physical, Analytical and Chemical Properties of Chiral Minerals

### 6.1. The Diastereomeric Interactions of Chiral Minerals with Polarized Light

Most of the physical properties of minerals, are dictated by their symmetry class, that is, the point-group component of their symmetry, including the detection of their chirality and the properties that are linked to chirality. As a general rule, in order to detect chirality, one has to use an analytical probe which itself is chiral. For instance, to identify that a glove is chiral, one probes it with one's left hand and then with the right hand, noticing that there are two distinctly different "interactions" between the glove and each of the hands. The fact that the two interactions are different, attests to the fact that the glove must be chiral. Furthermore, if one finds that, for instance, that the left hand interacts better with that glove, that may lead us to decide that the relevant handedness label of the glove should be "left" as well. If the object would have been achiral – say a sphere – then no difference in the interaction would have been recorded between a left- or right-hand holding it. The phenomenon of having left-probe/left-object and left-probe/right-object with different interactions (and likewise with right-probe/right-object and right-probe/left-object pairs) is called **diastereomerism**, and the different interactions - diastereomeric interactions. They appear in all of the enantioselective interactions: with polarized light as detailed in this Section, and with chiral molecules, as detailed next.

One of the most common features of chiral crystals is their ability to rotate linearly polarized light – the phenomenon of **optical rotation** (also sometimes referred to as optical activity). Relating to the hands and gloves example, linearly polarized light (also termed plane-polarized) can be envisioned as a superposition of two oppositely rotating circularly polarized light: One component

rotates to the right, the other to the left – that is, in a sense they are enantiomorphic polarizations. The enantiomorphism here is the helical sense of advancement of the circularly polarized component of electromagnetic field. Following the diastereomerism phenomenon just explained, left-handed and right-handed circularly polarized light interact differently with a chiral molecule or crystal, a phenomenon termed *circular birefringence* or *circular dichroism*. That difference leads to rotation of the vector of the linearly polarized light, clockwise (labeled as +, or dextrorotatory, or d) for one enantiomorph, and counterclockwise (minus, levorotatory, l) for the counter enantiomorph. The degree of optical rotation and even its sign, are dependent on the wavelength of measurement, and therefore reported optical rotations (polarimetry) state also the wavelength value. The optical rotation of crystals depends also on the orientation of the crystal, and therefore when comparing two enantiomorphs, the same orientation should be selected (for instance, the c-axis in the case of quartz).

The measurement of the optical rotation of several chiral minerals has been reported, starting with a long history of the optical rotation of quartz (Yogev-Einot and Avnir, 2006). Other examples of measurement of optical rotation of minerals include berlinite (Al(PO<sub>4</sub>) (Tanaka et al, 2010), cinnabar (HgS) (Chandrasekhar, 1953), sillenite (Bi<sub>12</sub>SiO<sub>20</sub>, I23) and more (Glazer and Stadnicka, 1986). We also mention here that ambers have optical rotation in the range of +15° to +25°, depending on the composition (Amber, <https://www.kremer-pigmente.com/elements/resources/products/files/60200e.pdf>). Polarimetry thus can be used as a simple tool for determining the authenticity of ambers.

The full graph of optical rotation as a function of wavelength is referred to as the *optical rotatory dispersion (ORD)* spectrum of the material – see as an example the ORD spectrum of quartz in Fig. 2 of (Buchen et al, 2019). The shape of that spectrum is a fingerprint of a chiral mineral, and can therefore be used as an analytical tool. The ORD spectra of the two enantiomorphs are mirror images of each other. Yet another spectral characterization of chiral crystals, especially in the visible range of light, is based on their circular dichroism property, namely that the intensity of absorbance of circularly polarized light, which is different for clockwise and counter-clockwise rotations of the polarized light. The spectrum of the difference between the two intensities of absorptions as a function of wavelength is termed the *circular dispersion (CD) spectrum*. For an example of such spectra, see the CD of HgS (cinnabar), Fig. 5 in (Vinegrad et al, 2018). As for the ORD spectrum, CD spectrum is characteristic for a given chiral mineral, and the CD spectra of a pair of enantiomorphs, are mirror images of each other.

The ORD and CD types of analysis highlights an important point: In general, one should bear in mind that *geometric chirality* (structural chirality) – as determined by crystallography or computationally - and *functional chirality* as determined by the outcome of a measurement of a physical or chemical property, are different concept; they are related, but geometric chirality does not always show up in a related chiral activity. For instance, in the ORD and CD spectra just discussed, there are cases where the spectrum crosses the zero point; that is, there are cases where if the measurement of the optical rotation or the CD signal of a chiral mineral at a certain specific wavelength, will be zero, despite of the existence of structural chirality. To generalize this point – a physical or chemical probe of chirality, does not always detect it. Furthermore, there is no inherent link between the handedness labeling of the crystallographic structure of an enantiomorph, and the handedness labeling attached to a physical outcome. Thus, the direction of optical rotation – plus (clockwise, dextrorotatory, d) or minus (anticlockwise, levorotatory, l) – has no relation to the crystallographic handedness label.

Linear polarizers and polarimetric imaging are routinely used for a variety of optical characterizations of crystals (Kaminsky et al, 2004). If (and only if) a chiral mineral belongs to the cubic crystal system (such as, for instance the gemstone mineral langbeinite, K<sub>2</sub>Mg<sub>2</sub>(SO<sub>4</sub>)<sub>3</sub>, P2<sub>1</sub>3), then the existence of its enantiomorphs can be detected by the use of crossed polarizers (Matsuura and Koshima, 2005; Meierhenrich, 2008).

## 6.2. The Interaction with X-rays and Electrons: Absolute Chiral Configuration Determination

A special, useful case of the diastereomeric interaction of circularly polarized electromagnetic irradiation with chiral crystals, is at the range of x-rays. It is a special method in x-ray crystallography which aims at the determination of the absolute configuration (the specific enantiomorph) of the chiral crystal, by comparative, diastereomeric analysis of the diffraction patterns obtained with left-handed and right-handed circularly polarized x-ray light (Valentín-Pérez et al, 2022). Examples of the use of this method for chiral minerals include berlinite ( $\text{AlPO}_4$ ,  $P3_121/P3_221$ ) (Tanaka et al, 2010), quartz (Tanaka et al, 2010; Tanaka et al, 2008), and the elemental chiral minerals of selenium and tellurium ( $P3_121/P3_221$ ) (Kozlovskaya et al, 2023).

However, while diastereomeric methods are the preferred way for identification of chirality, the use of circularly polarized X-rays is not trivial and is still not a common practice. Instead, approximate methods utilizing the diffraction of the standardly used unpolarized x-rays for determination of the absolute configuration have been developed; see for instance the absolute determination of the handedness of Te (Inui et al, 2006), and that of paratellurite,  $\alpha\text{-TeO}_2$  (as  $P4_12_12$  and not  $P4_32_12$ ) (Thomas, 1988) by such approximate methods. Particularly common is the use of Flack parameter for the absolute configuration determination with un-polarized x-rays (Watkin and Cooper, 2020), and in Section 3 we mentioned several cases of that use.

Diffraction for absolute structure determination is not limited to x-rays: diffraction of electrons for that purpose has been used as well. Thus, determination of the absolute configuration of quartz and tellurium enantiomorphs by various types of electron-diffraction analytical methods, has been reported (Winkelmann and Nolze, 2015; Dong and Ma, 2020; Goodman and Secomb, 1977). Similarly, electron diffraction enables the determination of the enantiomorph absolute structures in twins-laws, such as for Dauphine twins of quartz (McLaren and Phakey, 1969). Electrons are of course used in various electron microscopy methods, and indeed the use of aberration-corrected scanning TEM for the determination, again, of the enantiomorphs of quartz and tellurium, has been reported (Dong and Ma, 2020). Finally, diffraction of neutrons is used as well as a structural analytical tool, but I am unaware of the use of this technique for absolute configuration identification of mineral enantiomorphs. It has been used without enantiomorphs discrimination, for instance for the chiral mineral wardite ( $\text{NaAl}_3(\text{PO}_4)_2(\text{OH})_4 \cdot 2(\text{H}_2\text{O})$ ,  $P4_12_12/P4_32_12$ ) (Gatta et al, 2019) and for quartz (Wenk, 2006).

## 6.3. Physical Properties of Non-Centrosymmetric Crystals

In this section we extend the relation between the 11 chiral crystal classes and their physical properties to a larger class of crystal classes which includes the 11 chiral ones. The extended subdivision of the full list of 32 crystal classes is of classes that lack inversion element, but may have the other improper elements. Lacking inversion is a characteristic of chiral objects, but not only – there are additional classes which lack that symmetry element but have other improper elements in their space group, such as mirror symmetry. All of these are called the **non-centrosymmetric crystal classes**, and there are 21 classes of that type. In addition to the 11 chiral crystal classes, the rest 10 are the following achiral crystal classes:  $m$ ,  $mm2$ ,  $3m$ ,  $4mm$ ,  $6mm$ ,  $\bar{4}2m$ ,  $\bar{4}$ ,  $-6$ ,  $\bar{6}m2$  and  $\bar{4}3m$  (Glazer and Stadnicka, 1989). The rationale for this subdivision is that the non-centrosymmetric crystal classes share several key materials properties, which include the optical properties – optical rotation and optical second harmonic generation (an electromagnetic frequency doubling phenomenon) – and electric properties such as piezoelectricity (generation of an electric charge on crystal faces by application of mechanical stress), pyroelectricity (generation of electric potential by temperature changes), and ferroelectricity (reversibility of dipole moment affected by an applied voltage; all ferroelectrics are also piezoelectric and pyroelectric) (Ok et al, 2006).

Indeed, it turns out that optical rotation, described in the previous section, is not limited to chiral crystals, but may appear also in four crystal-classes belonging to the non-centrosymmetric crystal classes:  $\bar{4}$  ( $S_4$ ),  $m$  ( $C_s$ ),  $mm2$  ( $C_{2v}$ ) and  $\bar{4}2m$  ( $D_{2d}$ ) (Claborn et al, 2008). Focusing on the chiral crystal classes within the non-centrosymmetric classes, second harmonic generation, piezoelectricity and ferroelectricity are properties of all chiral crystal classes, except for the crystal class  $432$  ( $O$ ), and



pyroelectricity appears in 5 out of the 11 chiral crystal classes: 1 ( $C_1$ ), 2 ( $C_2$ ), 3 ( $C_3$ ), 4 ( $C_4$ ) and 6 ( $C_6$ ) (Halasyamani and Poeppelmeier, 1998).

Several chiral minerals already mentioned in this review have been subjected to measurements of the specific properties of the non-centrosymmetric classes. Perhaps the most studied case is quartz, because of its second harmonic generation property (Winta et al, 2018) and piezoelectric property (Labéguerie et al, 2010), the latter of which has given rise to the time-oscillator in quartz watches. Other chiral minerals in this review and in this category for which these electrical properties have been measured include epsomite ( $(\text{MgSO}_4 \cdot 7\text{H}_2\text{O}, P2_12_12_1)$  (Parkhomenko, 1971), the two phyllosilicate gemstones searlesite ( $\text{NaBSi}_2\text{O}_5(\text{OH})_2, P2_1$ ) and celadonite ( $\text{K}(\text{Mg}, \text{Fe}^{2+})(\text{Fe}^{3+}, \text{Al})[\text{Si}_4\text{O}_{10}](\text{OH})_2, C2$ ) (Piezoelectric Gems, [https://classicgems.net/info\\_Piezoelectricity.htm](https://classicgems.net/info_Piezoelectricity.htm)), berlinite ( $\text{Al}(\text{PO}_4), P3_121/P3_221$ ) (Hong et al, 1986), cancrinite ( $(\text{Na}, \text{Ca}, \square)_8(\text{Al}_6\text{Si}_6\text{O}_{24})(\text{CO}_3, \text{SO}_4)_2 \cdot 2\text{H}_2\text{O}, P6_3$ ) (Kobyakov et al, 1982), cinnabar ( $\text{HgS}, P3_121/P3_221$ ) and quartz (Fridkin et al, 2011); for comprehensive listings, see (Helman, 2016). As with the previously described methods, all of these additional properties can be used for authentication of the chirality of the mineral, and in fact, they can even be used for a more accurate determination of the relevant space group symmetry (centrosymmetric or not) in case of doubt (Loiacono et al, 1982).

#### 6.4. Surface Chirality: The Diastereomeric Interactions of Chiral Minerals with Chiral Molecules

The chemical interaction of a crystal with its surroundings is through its surface, and more precisely, through the various crystallographic planes, expressed in the specific habit. The molecular arrangement at these exposed crystallographic planes is a reflection of the 3D molecular structure, and is characterized by the atomic roughness of the plane, the atomic size steps and the corners. Although this is referred to as 2D chirality, it is actually a thin 3D surface roughness. Chiral crystals preserve chirality at their exposed surface, although of different atomic chiral shape (depending on the exposed crystallographic plane). Significantly, achiral crystals may display chiral 2D surfaces as well (Hazen, 2004; Downs and Hazen, 2004), and a mineral example is (achiral) calcite for which the 2D surface chirality was studied in detail (Hazen et al, 2001).

Yet another manifestation chirality of minerals at their surface, is the morphology of pits obtained by etching – there are cases of chiral minerals, where the morphology of etched pits of one enantiomorph are clearly mirror imaged in the counter enantiomorph. We already encountered such as case in Section 3 for nepheline ( $\text{Na}_3\text{KAl}_4\text{Si}_4\text{O}_{16}, P6_3$ ), for which the two enantiomorphs were identified from the morphologies of HCl-etching (Hejl and Finger, 2018). Likewise, the enantiomorphs of quartz are distinguishable by the patterns of etched triangular pits obtained by etching with hydrofluoric acid (Gault, 1949; Wilson, 1979).

From a practical point of view, for interfacial enantioselective chemical processes based on diastereomeric interactions between chiral molecules and chiral surfaces – adsorption, catalysis, chromatographic separation, etc. – single enantiomorph chiral crystals are used, as their handedness is not masked by the different exposed crystallographic planes. An example is the pronounced enantioselective adsorption of D-histidine over L-histidine on a single crystal of the chiral zeolitic mineral goosecreekite ( $\text{Ca}[\text{Al}_2\text{Si}_6\text{O}_{16}] \cdot 5\text{H}_2\text{O}, P2_1$ , as determined by sensitive calorimetry heats of adsorption measurements (Dryzun, 2009). The most studied mineral from the point of view of enantioselective adsorption is quartz. One of the main drives for this has been the idea that a slight excess of one of its enantiomorphs on planet Earth, was a driving force for the development of the homochirality of life on Earth. While that idea is not accepted anymore (because such slight excesses exist locally, they cancel out globally (Támara, and Preston, 2009), the field of enantioselective adsorptions has advanced due to it. An example is the observation by several groups, of the preferential adsorption of L-alanine (or its ester) on l-quartz which is confirmed by the expected “mirror” behavior, namely that D-alanine is adsorbed preferably on d-quartz (Kavasmaneck and Bonner, 1976).

Closely related to enantioselective adsorption on chiral crystals are enantioselective reactions, catalytic or not, which take place on the surface. Here, the handedness of the surface structure may dictate the handedness of the product chiral molecules (often involving an  $\text{Sp}^2$  carbon converted to

an  $Sp^3$  carbon). Nice examples were provided by Soai et al, who showed that the handedness of a catalytic reaction chiral product molecule - 5-pyrimidyl alkanol – was dictated by the specific handedness of quartz crystal (Soai et al,1999) or of cinnabar crystal, on the surfaces of which the reaction took place (Shindo et al, 2013).

#### 6.5. Property/Chirality Correlations: Quantifying the Degree of Chirality

Following the detection of chirality by any of the physical and chemical method described above, comes the following question: Is there a correlation between the “degree of chirality” and the degree of the intensity of the physical or chemical property that is linked to it? Traditionally, the concept of chirality has been treated in terms of either/or, that is, chirality either exists or not. However, intuition dictates that if a chiral structure is subjected to changes, for instance by pressure or temperature effects, then its degree of chirality will change as well, because the specific bond-lengths and bond angles will change. And, if a physical or chemical property is directly related to chirality – such as optical rotation – then a quantitative correlation should be detected between the level of that property and the degree of chirality. Following that intuition, we have developed a measure for the degree of chirality – the Continuous Chirality Measure (CCM) (Zabrodsky and Avnir, 1995) – which answers questions such as “by how much is one mineral more chiral than another one?” The CCM approach indeed revealed quantitative correlations in many domains of chemistry, biochemistry, physics, geology and materials science. The essence of that measure is the following: Find the minimal distance that the atoms of a given structure must move, in order to become achiral. If the distances are zero, then the object is achiral, and the measure is zero. It grows (up to 100) as the structure increases its distance from achirality. Now, since achirality means that the object has improper symmetry – reflection, in version, roto-inversion – the CCM is actually a measure of distortion from any of these symmetries (the minimal one), say from reflection. Indeed, the CCM is part of a more general Continuous Symmetry Measure (CSM) methodology (Zabrodsky et al, 1992) which answers questions such as “how much tetrahedrality exists in a given distorted tetrahedral structure?”; on the CSM scale, zero means that the structure has the exact symmetry, and it grows (up to 100), and the distortion from the analyzed symmetry grows. Computational tools are available free to the public (Tuvi-Arad et al, 2024). Here we briefly review of observations made with the CCM and CSM in the minerals’ world:

It turns out that the structures of the same mineral at different locations, are not necessarily the exact duplications of each other. The physical history of their formation, the local impurities, and so on, induce detectable variation in the structures. The CCM and CSM approaches were applied on crystallographic data of quartz samples from 13 different locations, by analyzing the degree of tetrahedrality (“T<sub>a</sub>-ness”) and chirality of the  $SiO_4$  building unit. It was found that the tetrahedrality measure of the  $SiO_4$  building block on the CSM scale varied for the 13 locations from 0.01 to 0.04, and that this distortion induced also a slight degree of chirality in that unit (up to 0.006 on the CCM scale). The induction of chirality is significantly more evident when the larger tetrahedron of the  $SiSi_4$  unit (that is, the  $Si(OSi)_4$  unit without the oxygen atoms) is taken – around 4.6 for all samples (Yogev-Einot and Avnir, 2003). Quartz was also the topic of a detailed study of the quantitative correlations between pressure and temperature (PT) and the degrees of chirality, of tetrahedral symmetry and of helicity (deviation from  $C_2$ -symmetry) that these PT changes induce. All of the main building units of quartz were taken, including  $SiO_4$ ,  $Si(OSi)_4$ ,  $SiSi_4$ , and the four  $SiO_4$  tetrahedra helix segment, - $O(SiO_3)_4$ -, for which a variety of monotonous correlation with PT were found (Yogev-Einot and Avnir, 2004). As mentioned above, pertoldite, a chiral polymorph of  $GeO_2$  is, isostructural with quartz, sharing the same space group. And indeed, it was found that the PT-chirality and symmetry correlations found for quartz, have the same trends for this mineral as well, and comparison of the degree of chirality of the various building blocks of quartz to those of pertoldite –  $GeO_2$ ,  $GeGe_4$  and - $O(GeO_3)_4$ -, showed that pertoldite is significantly more chiral than quartz (Yogev-Einot and Avnir, 2004).

An important observation made in that study was that is that CSM and CCM detect very sensitively the phase transition of alpha-quartz to beta-quartz at 846 K: The gradual change in these

measures as temperature is being raised, display a clear break at that point. The effect of changes in optical rotation and in degree of chirality due to temperature increase, was studied as well: In the late 19th century/beginning of the 20th, several researchers, the most famous of which is Le Chatelier, investigated the optical rotation changes of quartz with temperature. By employing the CCM methodology a remarkable agreement – near perfect overlap – between the original early optical rotation/temperature curve and the chirality/temperature curve, was shown. This provides a direct interpretation of the early observations, as reflecting the dependence of the optical rotation on the *degree* of chirality, linking these two properties quantitatively (Yogev-Einot and Avnir, 2006).

In all of the chirality/property relations described in this part, the link is with chirality, not with the handedness; a correlation with one enantiomorph will be mirror-imaged with the counter enantiomorph (such as change of sign or reversal of slope).

#### Data Sources

The leading data source has been mainly Mindat, <https://www.mindat.org/>. Several other major sources which have been used intensively as well:

\* Wikipedia, by mineral name. Partial lists of minerals by space group appear at [https://en.wikipedia.org/wiki/Category:Minerals\\_in\\_space\\_group\\_XXX](https://en.wikipedia.org/wiki/Category:Minerals_in_space_group_XXX).

\* IMA's <https://rruff.info/ima/>. For instructions of how to use it see <sup>Note 8</sup>.

\* Webmineral, <https://www.webmineral.com/>. Lists of minerals by their crystal class: <https://webmineral.com/crystall.shtml>

\* American Mineralogist Crystal Structure Database, <https://rruff.geo.arizona.edu/AMS/amcsd.php>

\* Handbook of Mineralogy, <https://handbookofmineralogy.org/>.

Lists of the chiral minerals within each class can be found at <https://webmineral.com/crystall.shtml> and <https://www.mindat.org/crystalsystems.php>.

Mineral listings occasionally do not agree on compositions or space-group symmetries. For instance, while Mindat describes combeite as an achiral  $\text{Na}_{4.5}\text{Ca}_{3.5}\text{Si}_6\text{O}_{17.5}(\text{OH})_{0.5}$  mineral at space group  $R\bar{3}m$ , webmineral data base describes this mineral as chiral  $\text{Na}_2\text{Ca}_2\text{Si}_3\text{O}_9$  at space group  $P3_121/P3_221$ . For consistency I usually took Mindat's version on such occasions.

References to all minerals listed in the tables and in the text listings, can be found in Mindat specific entries, in "The New IMA List of Minerals", July 2024, <https://mineralogy-ima.org/Minlist.htm>, and in the other sources mentioned above.

The order follows Table 1. The minerals are grouped in pairs of enantiomorphic space groups. In most cases only one enantiomorphic mineral is described and the dash means "either-or". The minerals that do have the two enantiomorphs reported, are in **bold**, and are described in the text.

#### P<sub>4</sub>1 - P<sub>4</sub>3:

Percleveite-(La),  $\text{La}_2\text{Si}_2\text{O}_7$

Percleveite-(Ce),  $\text{Ce}_2\text{Si}_2\text{O}_7$

#### P<sub>4</sub>122 - P<sub>4</sub>322:

Lemanskiite,  $\text{NaCaCu}_5(\text{AsO}_4)_4\text{Cl}\cdot 3\text{H}_2\text{O}$

Manganoquadratite,  $\text{AgMnAsS}_3$

Quadratite,  $\text{Ag}(\text{Cd,Pb})\text{AsS}_3$

#### P<sub>4</sub>12<sub>1</sub>2 - P<sub>4</sub>32<sub>1</sub>2

Cristobalite,  $\text{SiO}_2$  (quartz polymorph)

Cuprotungstite,  $\text{Cu}_2(\text{WO}_4)(\text{OH})_2$

**Cyrllovite**,  $\text{NaFe}^{3+}_3(\text{PO}_4)_2(\text{OH})_4\cdot 2\text{H}_2\text{O}$

Fluorowardite,  $\text{NaAl}_3(\text{PO}_4)_2\text{F}_2(\text{OH})_2(\text{H}_2\text{O})_2$

Kamphaugite-(Y),  $\text{Ca}_2\text{Y}_2(\text{CO}_3)_4(\text{OH})_2\cdot 3\text{H}_2\text{O}$

Keatite,  $\text{SiO}_2$  (quartz polymorph)

Lipscombite,  $\text{Fe}^{2+}\text{Fe}^{3+}_2(\text{PO}_4)_2(\text{OH})_2$

Maucherite,  $\text{Ni}_{11}\text{As}_8$

Paratellurite,  $\alpha\text{-TeO}_2$

Retgersite,  $\text{NiSO}_4\cdot 6\text{H}_2\text{O}$

Sweetite,  $\text{Zn}(\text{OH})_2$   
 Ungavaite,  $\text{Pd}_4\text{Sb}_3$   
 Wardite,  $\text{NaAl}_3(\text{PO}_4)_2(\text{OH})_4 \cdot 2\text{H}_2\text{O}$   
 Wuyanzhiite,  $\text{Cu}_2\text{S}$   
 Zinclipscornbite,  $\text{ZnFe}^{3+}_2(\text{PO}_4)_2(\text{OH})_2$   
P31 – P32  
 Monohydrocalcite,  $\text{CaCO}_3 \cdot \text{H}_2\text{O}$   
 Sheldrickite,  $\text{NaCa}_3(\text{CO}_3)_2\text{F}_3 \cdot \text{H}_2\text{O}$   
 Stavelotite-(La),  $\text{La}_3\text{Mn}^{2+}_3\text{Cu}^{2+}(\text{Mn}^{3+}, \text{Fe}^{3+}, \text{Mn}^{4+})_{26}(\text{Si}_2\text{O}_7)_6\text{O}_{30}$   
 Stillwellite-(Ce),  $(\text{Ce}, \text{La}, \text{Ca})\text{BSiO}_5$   
P312 – P3212  
 Caresite,  $\text{Fe}^{2+}_4\text{Al}_2(\text{OH})_{12}[\text{CO}_3] \cdot 3\text{H}_2\text{O}$   
 Müllerite,  $\text{Pb}_2\text{Fe}^{3+}(\text{Te}^{6+}\text{O}_6)\text{Cl}$   
 Muscovite-3T,  $\text{KAl}_2(\text{AlSi}_3\text{O}_{10})(\text{OH})_2$  (a mica 3T polytype)  
P3121 – P3221  
 Alarsite,  $\text{AlAsO}_4$   
 Bassanite,  $2\text{CaSO}_4 \cdot \text{H}_2\text{O}$  check anhydrous  
 Berlinite,  $\text{AlPO}_4$   
**Cinnabar**,  $\text{HgS}$   
 Eliopouosite,  $\text{V}_7\text{S}_8$

Faheyite,  $\text{Be}_2\text{Mn}^{2+}\text{Fe}^{3+}_2(\text{PO}_4)_4 \cdot 6\text{H}_2\text{O}$

Ingersonite,  $\text{Ca}_3\text{Mn}^{2+}\text{Sb}^{5+}_4\text{O}_{14}$   
 Matildite,  $\text{AgBiS}_2$   
 Norilskite,  $(\text{Pd}, \text{Ag})_{2x}\text{Pb}$  ( $x=0.08-0.11$ )  
 Quartz,  $\text{SiO}_2$   
 Rhabdophane-(Ce),  $\text{Ce}(\text{PO}_4) \cdot 0.6\text{H}_2\text{O}$   
 Rodolicoite,  $\text{Fe}^{3+}\text{PO}_4$   
 Schuetteite,  $\text{Hg}^{2+}_3(\text{SO}_4)\text{O}_2$   
**Selenium**, Se  
**Tellurium**, Te  
 Zirconolite-3T,  $(\text{Ca}, \text{REE})_2\text{Zr}_2(\text{Ti}, \text{Nb})_3\text{FeO}_{14}$   
 Ximengite,  $\text{BiPO}_4$   
P61 – P65  
 Nagelschmidtite,  $\text{Ca}_7(\text{SiO}_4)_2(\text{PO}_4)_2$   
 Trinepheline,  $\text{NaAlSiO}_4$   
P62 – P64  
 Apparently not reported  
P6122 – P6522  
 Apparently not reported  
P6222 – P6422  
 The Rhabdophane Group:  
 Brockite,  $(\text{Ca}, \text{Th}, \text{Ce})\text{PO}_4 \cdot \text{H}_2\text{O}$   
 Grayite,  $(\text{Th}, \text{Pb}, \text{Ca})(\text{PO}_4) \cdot \text{H}_2\text{O}$   
 Rhabdophane-(La),  $\text{La}(\text{PO}_4) \cdot \text{H}_2\text{O}$   
 Rhabdophane-(Nd),  $\text{Nd}(\text{PO}_4) \cdot \text{H}_2\text{O}$   
 Rhabdophane-(Y),  $\text{YPO}_4 \cdot \text{H}_2\text{O}$   
 Smirnovskite,  $(\text{Th}, \text{Ca})\text{PO}_4 \cdot n\text{H}_2\text{O}$   
 Tristramite,  $(\text{Ca}, \text{U}, \text{Fe})(\text{PO}_4, \text{SO}_4) \cdot 2\text{H}_2\text{O}$   
 UM1993-07-PO:CaCeHLA,  $(\text{Ca}, \text{Ce}, \text{La}, \text{REE})\text{PO}_4 \cdot n\text{H}_2\text{O}$   
 Tounkite,  $(\text{Na}, \text{Ca}, \text{K})_8(\text{Al}_6\text{Si}_6\text{O}_{24})(\text{SO}_4)_2\text{Cl} \cdot \text{H}_2\text{O}$   
 Virgilite,  $\text{LiAlSi}_2\text{O}_6$   
P4132 – P4332



Cholalite,  $(\text{Cu,Sb})_3(\text{Pb,Ca})_3(\text{TeO}_3)_6\text{Cl}$

Coldwellite,  $\text{Pd}_3\text{Ag}_2\text{S}$

**Maghemite**  $\text{Fe}_2\text{O}_3$ ,  $\gamma\text{-Fe}_2\text{O}_3$  ( $(\text{Fe}^{3+}_{0.67}\square_{0.33})\text{Fe}^{3+}_2\text{O}_4$ )

Titanomaghemite,  $(\text{Ti}^{4+}_{0.5}\square_{0.5})\text{Fe}^{3+}_2\text{O}_4$

The Table reads as follows: # group number: group symbol (number of minerals in that group), mineral name, chemical composition. The 10 top most populated space-groups of chiral minerals, are **bolded**.

#1: **P1 (80)**, babefphite,  $\text{BaBe}(\text{PO}_4)(\text{F,OH})$

#3: P2 (9), zippeite,  $\text{K}_4(\text{UO}_2)_6(\text{SO}_4)_3(\text{OH})_{10}\cdot 4(\text{H}_2\text{O})$

#4: **P2<sub>1</sub> (50)**, uranophane,  $(\text{Ca}(\text{UO}_2)_2(\text{SiO}_3\text{OH})_2\cdot 5\text{H}_2\text{O})$

#5: **C2 (31)**, campigliaite,  $\text{Cu}_4\text{Mn}(\text{SO}_4)_2(\text{OH})_6\cdot 4\text{H}_2\text{O}$

#16: P222 (3), zýkaite,  $\text{Fe}^{3+}_4(\text{AsO}_4)_3(\text{SO}_4)(\text{OH})\cdot 15\text{H}_2\text{O}$

#17: P222<sub>1</sub> (1), achyrophanite,  $(\text{K,Na})_3(\text{Fe}^{3+},\text{Ti,Al,Mg})_5\text{O}_2(\text{AsO}_4)_5$

#18: P2<sub>1</sub>2<sub>1</sub>2 (7), sussexite,  $\text{Mn}^{2+}\text{BO}_2(\text{OH})$

#19: **P2<sub>1</sub>2<sub>1</sub>2<sub>1</sub> (51)**, teineite,  $\text{Cu}(\text{TeO}_3)\cdot 2\text{H}_2\text{O}$

#20: C222<sub>1</sub> (11), seeligerite,  $\text{Pb}_3\text{Cl}_3(\text{IO}_3)\text{O}$

#21: C222 (2), jarosewichite,  $\text{Mn}^{2+}_3\text{Mn}^{3+}(\text{AsO}_4)(\text{OH})_6$

#22: F222 (1), pseudograndreefite,  $\text{Pb}_6(\text{SO}_4)\text{F}_{10}$

#23: I222 (0); #24: I2<sub>1</sub>2<sub>1</sub>2<sub>1</sub> (0); #75: P4 (0); #77: P4<sub>2</sub> (0)

#79: I4 (2), piypite,  $\text{K}_2\text{Cu}_2\text{O}(\text{SO}_4)_2$

#80: I4<sub>1</sub> (0); #89: P422 (0); #90: P42<sub>1</sub>2 (0); #93: P4<sub>2</sub>22 (0); #94: P4<sub>2</sub>2<sub>1</sub>2 (0)

#97: I422 (1), ekanite,  $\text{Ca}_2\text{ThSi}_8\text{O}_{20}$

#98: I4<sub>1</sub>22 (1), biphosphammite,  $\text{NH}_4(\text{H}_2\text{PO}_4)$

#143: **P3 (26)**, marathonite,  $\text{Pd}_{25}\text{Ge}_9$

#146: **R3 (26)**, bluebellite,  **$\text{Cu}_6[(\text{I}^{5+}\text{O}_3)(\text{OH})_3](\text{OH})_7\text{Cl}$**

#149: P312 (3), backite  $\text{Pb}_2\text{AlTeO}_6\text{Cl}$

#150: **P321 (17)**, qeltite,  $\text{Ca}_3\text{TiSi}_2(\text{Fe}^{3+}_2\text{Si})\text{O}_{14}$

#155: **R32 (14)**, abhurite,  **$\text{Sn}_{21}\text{Cl}_{16}(\text{OH})_{14}\text{O}_6$**

#168: P6 (1), ekaterinite,  $\text{Ca}_2(\text{B}_4\text{O}_7)(\text{Cl,OH})_2\cdot 2\text{H}_2\text{O}$

#173: **P6<sub>3</sub> (43)**, zinkenite,  **$\text{Pb}_9\text{Sb}_{22}\text{S}_{42}$**

#177: P622 (2), currierite,  $\text{Na}_4\text{Ca}_3\text{MgAl}_4(\text{AsO}_3\text{OH})_{12}\cdot 9\text{H}_2\text{O}$

#182: P6<sub>3</sub>22 (8), kalsilite,  $\text{KAlSiO}_4$

#195: **P23 (0)**

#196: F23 (1), tululite,  $\text{Ca}_{14}(\text{Fe}^{3+},\text{Al})(\text{Al,Zn,Fe}^{3+},\text{Si,P,Mn,Mg})_{15}\text{O}_{36}$

#197: I23 (3), wilancookite,  $(\text{Ba}_5\text{Li}_2\square)\text{Ba}_6\text{Be}_{24}\text{P}_{24}\text{O}_{96}\cdot 26\text{H}_2\text{O}$

#198: **P2<sub>1</sub>3 (19)**, naquite,  **$\text{FeSi}$**

#199: I2<sub>1</sub>3 (4), corderoite,  $\text{Hg}_3\text{S}_2\text{Cl}_2$

#207: P432 (0); #208: P4<sub>2</sub>32 (0); #209: F432 (0); #210: F4<sub>1</sub>32 (0); #211: I432 (0)

#214: I4<sub>1</sub>32 (4), ye'elimite,  $\text{Ca}_4\text{Al}_6\text{O}_{12}(\text{SO}_4)$

## References

- Addadi, L., Geva, M. 2003. Molecular recognition at the interface between crystals and biology: generation, manifestation and detection of chirality at crystal surfaces Cryst. Eng. Comm. 5, 140–146 DOI: 10.1039/b304061e
- Amber, <https://www.mindat.org/min-188.html>
- Amber, <https://www.kremer-pigmente.com/elements/resources/products/files/60200e.pdf>
- Armstrong, D.W. et al, 1996. Enantiomeric composition and prevalence of some bicyclic monoterpenoids in amber. Chirality 8, 39 – 48. DOI:10.1002/(SICI)1520-636X(1996)8:1<39::AID-CHIR9>3.0.CO;2-B
- Austinite, <https://en.wikipedia.org/wiki/Austinite>
- Avnir, D., Editor, 1989. The Fractal Approach to Heterogeneous Chemistry: Surfaces, Colloids, Polymers. Wiley, Chichester, 1989. 3rd printing: 1992.
- Avnir, D., Huylebrouck, D. 2013. On Left and Right: Chirality in Architecture. Nexus Network Journal: Architecture and Mathematics 15, 171-182. DOI 10.1007/s00004-013-0144-x

- Avnir, D., 2021. Critical review of chirality indicators of extraterrestrial life. *New Astronomy Rev.* 92, 101596. <https://doi.org/10.1016/j.newar.2020.101596>
- Avrahami, E.M., 2022. Complex morphologies of biogenic crystals emerge from anisotropic growth of symmetry-related facets. *Science* 376, 312–316. DOI: 10.1126/science.abm1748
- Bayliss, P., 1982. A further crystal structure refinement of gersdorffite. *American Mineralogist* 67, 1058–1064. Beta-Tridymite, <https://www.mindat.org/min-47886.html>
- Bouropoulos, N. et al, 2001. Calcium oxalate crystals in tomato and tobacco plants: morphology and in vitro interactions of crystal-associated macromolecules. *Chemistry A Europ. J.* 7, 1881–1888. doi: 10.1002/1521-3765(20010504)7:9<1881::aid-chem1881>3.0.co;2-i.
- Bouska, V., et al, 1998. Hartite from Bilina. *American Mineralogist* 83, 1340–1346. <https://doi.org/10.2138/am-1998-11-1224>
- Buchen, J. et al, 2019. Twins in  $YAl_3(BO_3)_4$  and  $K_2Al_2B_2O_7$  crystals as revealed by changes in optical activity. *Crystals* 9, 8. doi:10.3390/cryst9010008
- Cambridge Structural Database, <https://www.ccdc.cam.ac.uk/media/CSD-Space-Group-Statistics-Space-Group-Number-Ordering-2024.pdf>
- Carbon Mineral Challenge, [https://en.wikipedia.org/wiki/Carbon\\_Mineral\\_Challenge](https://en.wikipedia.org/wiki/Carbon_Mineral_Challenge)
- Carretero-Genevri, A. et al, 2015. Chiral habit selection on nanostructured epitaxial quartz films. *Faraday Discuss.*, 179, 227–233. DOI: 10.1039/c4fd00266k
- Chandrasekhar, S., 1953. The optical rotatory dispersion of cinnabar. *Proc. Indian Acad. Sci.* 37, 697–703. <https://doi.org/10.1007/BF03052697>
- Chemicool Dictionary, [https://www.chemicool.com/definition/lattice\\_crystal.html](https://www.chemicool.com/definition/lattice_crystal.html)
- Claborn, K. et al, 2008. Optical Rotation of Achiral Compounds. *Angew. Chem. Int. Ed.* 47, 5706 – 5717. DOI: 10.1002/anie.200704559
- Cody, A.M., Cody, R.D., 1991. Chiral habit modifications of gypsum from epitaxial-like adsorption of stereospecific growth inhibitors. *Journal of Crystal Growth* 113, 508–519. DOI:10.1016/0022-0248(91)90086-K
- Cooper, M. et al, 2000. Refinement of the crystal structure of cyrilovite from Cyrilov, Western Moravia, Czech Republic. *Journal of the Czech Geological Society*, 45, 95 - 100
- Crystalografia, [https://www.xtal.iqf.csic.es/Cristalografia/parte\\_03\\_4-en.html](https://www.xtal.iqf.csic.es/Cristalografia/parte_03_4-en.html)
- Cyrilovite, <https://gemstone.fandom.com/wiki/Cyrilovite>
- Dapiaggi, M., 2015. The formation of silica high temperature polymorphs from quartz: Influence of grain size and mineralising agents. *Journal of the European Ceramic Society* 35, 4547–4555. <http://dx.doi.org/10.1016/j.jeurceramsoc.2015.08.015>
- Damien Daval, D., 2018. Carbon dioxide sequestration through silicate degradation and carbon mineralisation: promises and uncertainties. *npj Materials Degradation* 2, 11. doi:10.1038/s41529-018-0035-4
- Disphenoid, <https://en.wikipedia.org/wiki/Disphenoid>
- Dong, Z., Ma, Y., 2020. Atomic-level handedness determination of chiral crystals using aberration-corrected scanning transmission electron microscopy. *Nature Commun.* 11, 1588. <https://doi.org/10.1038/s41467-020-15388-5>
- Downs, R.T., Hazen, R.M., 2004. Chiral indices of crystalline surfaces as a measure of enantioselective potential. *J. Mol. Catal. A Chem.* 216, 273–285. <https://doi.org/10.1016/j.molcata.2004.03.026>
- Drewitt, J.W.E et al, 2022. From short to medium range order in glasses and melts by diffraction and Raman spectroscopy. *Reviews in Mineralogy and Geochemistry* 87, 55–103. <https://doi.org/10.2138/rmg.2022.87.02>
- Drees, L.R. et al, 1989. Silica in Soils: Quartz and Disordered Silica Polymorphs. Chapter 19 in *Minerals in Soil Environments*, Volume 1, Editors: Dixon, J.B., Weed, S.B. The Soil Science Society of America, Inc. <https://doi.org/10.2136/sssabookser1.2ed.c19>
- Dryzun, C., Avnir, D., 2012. On the abundance of chiral crystals. *Chem. Commun.* 48, 5874–5876. DOI: 10.1039/c2cc17727g
- Dryzun, C. et al., 2009. Chiral silicate zeolites. *J. Mater. Chem.* 19, 2062–2069. DOI:10.1039/b817497k
- Erez, J., 2003. The source of ions for biomineralization in foraminifera and their implications for paleoceanographic proxies. *Reviews in Mineralogy and Geochemistry* 54, 115–149. <https://doi.org/10.2113/0540115>
- External Symmetry of Crystals, 32 Crystal Classes, <https://www2.tulane.edu/~sanelson/eens211/32crystalclass.htm>
- Fabián, L., Brock, C.P., 2010. A list of organic kryptoracemates. *Acta Crystallogr. B* 66, 94–103. doi: 10.1107/S0108768109053610
- Flack H.D., 2003. Chiral and achiral crystal structures. *Helvetica Chim. Acta* 86, 905–921. <https://doi.org/10.1002/hlca.200390109>
- Fortes, A.D. 2005. From Surrey to the moons of Jupiter (via Mars): The story of epsomite. *Axis*, 1, 1–28. <https://mineralogicalrecord.com/wp-content/uploads/2020/10/pdfs/Epsomite-Article-Figs.pdf>

- V. M. Fridkin, V.M. et al, 1982. The linear and circular bulk photovoltaic effect in piezoelectric crystals  $\text{Er}(\text{HCOO})_3 \cdot 2\text{H}_2\text{O}$  and  $\text{HgS}$ . *Ferroelectrics* 44, 27- 31. <https://doi.org/10.1080/00150198208260640>
- Friis, H., Balic-Zunic, T., 2005. Complex twinning and incorporation of REE into leucophanite. In *CER200 – Rare earth minerals*, GFF, 127:1, 35. DOI: 10.1080/11035890501271033
- Gatta, G.D., et al, 2019. A single-crystal neutron diffraction study of wardite,  $\text{NaAl}_3(\text{PO}_4)_2(\text{OH})_4 \cdot 2\text{H}_2\text{O}$ . *Phys Chem Minerals* 46, 427–435. <https://doi.org/10.1007/s00269-018-1013-7>
- Gault, H.R., 1949. The frequency of twin types in quartz crystals. *American Mineralogist* 34, 142–162. [http://www.minsocam.org/msa/collectors\\_corner/arc/qtztwin.htm](http://www.minsocam.org/msa/collectors_corner/arc/qtztwin.htm)
- Glassy igneous rock, <https://www.mindat.org/min-50714.html>
- Glazer, A.M., 2018. Confusion over the description of the quartz structure yet again. *J. Appl. Cryst.* 51, 915–918. <https://doi.org/10.1107/S160057671800434X>
- Glazer, A.M., Stadnicka, K., 1986. On the origin of optical activity in crystal structures. *J. Appl. Cryst.* 19, 108–122. <https://doi.org/10.1107/S0021889886089823>
- Glazer, A.M., Stadnicka, K., 1989. On the Use of the Term 'Absolute' in Crystallography. *Acta Cryst. A* 45, 234–238. <https://doi.org/10.1107/S0108767388011055>
- Goodman, P., Secomb, T.W., 1977. Identification of enantiomorphously related space groups by electron diffraction. *Acta Cryst. A* 33, 126–133. <https://doi.org/10.1107/S0567739477000266>
- Goslarite Mineral Data, <https://webmineral.com/data/Goslarite.shtml>
- Götze, J. et al., 2021. Mineralogy and mineral chemistry of quartz: A review. *Mineralogical Magazine* 85, 639–664. doi:10.1180/mgm.2021.72
- Hahn, Th., Klapper, H., 2006. Tables 10.1.2.2 and 10.1.2.3 in *International Tables for Crystallography Vol. A*, Section 10.1.2, pp. 771 and 791. <https://doi.org/10.1107/97809553602060000520>
- Hahn, Th. et al, 2016. Table 3.2.1.3 in *International Tables for Crystallography (2016)*, Vol. A, p.724. <https://onlinelibrary.wiley.com/iucr/itc/Ac/contents/>
- Halasyamani, P.S., and Kenneth R. Poeppelmeier, K.R., 1998. Noncentrosymmetric oxides. *Chem. Mater.* 10, 2753–2769. <https://doi.org/10.1021/cm980140w>
- Hatch, D.M., Ghose, S., 1991. The a-b Phase Transition in Cristobalite,  $\text{SiO}_2$ . *Phys. Chem. Minerals* 17, 554–562
- Hazen, R.M. et al, 2001. Selective adsorption of L- and D-amino acids on calcite: Implications for biochemical homochirality. *PNAS* 98, 5487–5490. [www.pnas.org/ycgi/doi/10.1073/pnas.101085998](http://www.pnas.org/ycgi/doi/10.1073/pnas.101085998)
- Hazen, R.M., 2004. Chiral crystal faces of common rock-forming minerals. Chapter 11 in *Progress in Biological Chirality*, Palyi, G. et al, Eds. Oxford: Elsevier, pp.137–151
- Hazen, R.M. et al, 2009. Evolution of uranium and thorium minerals. *American Mineralogist* 94, 1293–1311. DOI: 10.2138/am.2009.3208 1293
- Hazen, R.M. et al, 2016. Carbon mineral ecology: Predicting the undiscovered minerals of carbon. *American Mineralogist* 101, 889–906. DOI: <http://dx.doi.org/10.2138/am-2016-5546>
- Hazen, R.M., 2019. *Symphony in C: Carbon and the Evolution of (Almost) Everything*. W. W. Norton & Company
- Hazen, R.M. et al, 2022. On the paragenetic modes of minerals: A mineral evolution perspective. *American Mineralogist* 107, 1262–1287. DOI: <https://doi.org/10.2138/am-2022-8099>
- Hejl, E., Finger, F. 2018. Chiral Proportions of Nepheline Originating from Low-Viscosity Alkaline Melts. A Pilot Study. *Symmetry* 10, 410. doi:10.3390/sym10090410
- Helman, D.S., 2016. Symmetry-based electricity in minerals and rocks: A review with examples of centrosymmetric minerals that exhibit pyro and piezoelectricity. *Periodico di Mineralogia* 85, 201–248. DOI: 10.2451/2016PM590
- Hoffmann, F., 2016. Introduction to Crystallography. Springer Fachmedien Wiesbaden GmbH. <https://doi.org/10.1007/978-3-030-35110-6>
- Hoffmann, F. Frank Hoffmann, <https://www.youtube.com/@FrankHoffmann1000>
- Hong, W. et al 1986. The piezoelectric and elastic properties of berlinite and the effect of defects on the physical properties. *Journal of Crystal Growth* 79, 227–231. [https://doi.org/10.1016/0022-0248\(86\)90442-2](https://doi.org/10.1016/0022-0248(86)90442-2)
- Hongu, H., et al, 2019. Crystal structure and XANES investigation of petzite,  $\text{Ag}_3\text{AuTe}_2$ . *Acta Cryst. B* 75, 273–278. <https://doi.org/10.1107/S2052520619002166>
- Horwell, C.J. et al, 2013. The nature and formation of cristobalite at the Soufrière Hills volcano, Montserrat: implications for the petrology and stability of silicic lava domes. *Bull Volcanol* (2013) 75:696 DOI 10.1007/s00445-013-0696-3
- Huang, T-Y., et al, 2024. Recent progress in chiral zeolites: Structure, synthesis, characterization and applications, *Chinese Chemical Letters*, in press. doi: <https://doi.org/10.1016/j.ccl.2024.109758>
- Hummer, D.R. et al, 2022. Evidence for the oxidation of Earth's crust from the evolution of manganese minerals. *Nature Commun.* 13, 960. <https://doi.org/10.1038/s41467-022-28589-x>

- Iggland, M., Mazzotti, M., 2011. A population balance model for chiral resolution via Viedma ripening. *Cryst. Growth Des.* 11, 4611–4622. dx.doi.org/10.1021/cg2008599
- Inui, H. et al, 2007. Enantiomorph identification of crystals belonging to the point groups 321 and 312 by convergent-beam electron diffraction. *J. Appl. Cryst.* 40, 241–249. doi:10.1107/S0021889806055877
- Jiang, W. et al, 2019. Homochirality in biomineral suprastructures induced by assembly of single-enantiomer amino acids from a nonracemic mixture. *Nature Commun.* 10, 2318. <https://doi.org/10.1038/s41467-019-10383-x>
- Kaminsky, W. et al, 2004. Polarimetric imaging of crystals. *Chem. Soc. Rev.* 33, 514–525. DOI <https://doi.org/10.1039/B201314M>
- Kaolinite Subgroup, <https://www.mindat.org/min-43755.html>
- Katzenelson, O. et al. 1996. Chirality of large random supramolecular structures. *Chemistry - A European J.* 2, 174 – 181. <https://doi.org/10.1002/chem.19960020209>
- Kavasmaneck, P.R., Bonner, W.A., 1977. Adsorption of amino acid derivatives by d- and l-quartz. *Journal of the American Chemical Society* 99, 44-50. <https://doi.org/10.1021/ja00443a011>
- I. B. Kobayakov, I.B. et al, 1982. On a peculiarity of the piezoeffect in carbonate-cancrinite crystals. *Sov. Phys. JETP* 56, 1112-1115.
- Kozlovskaya, K.A. et al, 2023. Determination of the absolute configuration of monoatomic chiral crystals using three-wave X-ray diffraction. *Crystallography Reports* 68, 374–379. DOI: 10.1134/S1063774523700050
- Kremer, D. et al, 2022. Separation of reaction products from ex-situ mineral carbonation and utilization as a substitute in cement, paper, and rubber applications. *Journal of CO<sub>2</sub> Utilization* 62, 102067. <https://doi.org/10.1016/j.jcou.2022.102067>
- Labéguerie, P. et al, 2010. Structural, electronic, elastic, and piezoelectric properties of  $\alpha$ -quartz and  $MXO_4$  ( $M=Al, Ga, Fe; X=P, As$ ) isomorph compounds: A DFT study. *Phys. Rev. B* 81, 045107. DOI : 10.1103/PhysRevB.81.045107
- Lee, C. et al, 2022. Chirality in organic and mineral Systems: A review of reactivity and alteration processes relevant to prebiotic chemistry and life detection missions. *Symmetry* 14, 460. <https://doi.org/10.3390/sym14030460>
- List of gemstones by species, [https://en.wikipedia.org/wiki/List\\_of\\_gemstones\\_by\\_species](https://en.wikipedia.org/wiki/List_of_gemstones_by_species) and other listings
- Loiacono, G.M. et al, 1982. Resolution of space group ambiguities in minerals. *American Mineralogist* 67, 846–847.
- Liu, X-H et al, 2023. Genetic significance of trace elements in hydrothermal quartz from the Xiangzhong metallogenic province, South China. *Ore Geology Reviews* 152, 105229. <https://doi.org/10.1016/j.oregeorev.2022.105229>
- Mace, H.A., Peterson, R.C., 1995. The crystal structure of fichtelite, a naturally occurring hydrocarbon. *Can. Mineral.*, 33, 7–11.
- Matsuura, T., Koshima, H., 2005. Introduction to chiral crystallization of achiral organic compounds. Spontaneous generation of chirality. *Journal of Photochemistry and Photobiology C: Photochemistry Reviews* 6, 7–24. doi:10.1016/j.jphotochemrev.2005.02.002
- McLaren, A.C., Phakey, P.P., 1969. Diffraction contrast from Dauphine twin boundaries in quartz. *Phys. Stat. Sol.* 31, 723-737. <https://doi.org/10.1002/pssb.19690310233>
- Meierhenrich, U., 2008. Note 4, p.64 in *Amino Acids and the Asymmetry of Life*. *Advances in Astrobiology and Biogeophysics*. Springer-Verlag Berlin Heidelberg
- Nassau, K., 1978. The origins of color in minerals. *American Mineralogist* 63, 219-229
- Ng, H.N., C. Calvo, C., 1976. X-ray study of the  $\alpha$ - $\beta$  transformation of berlinite ( $AlPO_4$ ). *Canadian Journal of Physics* 54, 638-647. <https://doi.org/10.1139/p76-070>
- Ok, K.M. et al, 2006. Bulk characterization methods for non-centrosymmetric materials: second harmonic generation, piezoelectricity, pyroelectricity, and ferroelectricity. *Chem. Soc. Rev.* 35, 710–717. DOI: 10.1039/b511119f
- Overview of Silica Polymorphs, [http://www.quartzpage.de/gen\\_mod.html](http://www.quartzpage.de/gen_mod.html)
- E. I. Parkhomenko, E.I., 1971. Piezoelectric and Pyroelectric Effects in Minerals, in *Electrification Phenomena in Rocks*, Chapter 2. Springer Science+Business Media New York
- Pažout, R. et al, 2018. Refikite from Krásno, Czech Republic: a crystal-and molecular-structure study *Mineralogical Magazine* 79, 59 – 70. DOI: <https://doi.org/10.1180/minmag.2015.079.1.06>
- Perkins, D., et al, 2023. Forms and Point Groups. Section 10.5.1 in *Mineralogy*, LibreTextsTM. [https://geo.libretexts.org/Bookshelves/Geology/Mineralogy\\_\(Perkins\\_et\\_al.\)](https://geo.libretexts.org/Bookshelves/Geology/Mineralogy_(Perkins_et_al.))
- Piezoelectric Gems, [https://classicgems.net/info\\_Piezoelectricity.htm](https://classicgems.net/info_Piezoelectricity.htm)
- Petríček, V. et al, 1990. Orientational disorder in phenanthrene. Structure determination at 248, 295, 339 and 344 K. *Acta Cryst. B* 46, 830-832. DOI: 10.1107/S0108768190007510 *Acta*
- Pinto, Y. et al, 1966. Continuous chirality analysis of interconversion pathways of the water-trimer enantiomers. *J. Chem Soc. Faraday Trans.* 92, 2523 – 2527.



- Pinto Y, Avnir D., 2001. A generalized handedness labeling strategy: Addressing latent handedness in chiral structures. *Enantiomer* 6, 211-217.
- Pogge von Strandmann, P.A.E., et al 2019. Rapid CO<sub>2</sub> mineralisation into calcite at the CarbFix storage site quantified using calcium isotopes. *Nature Commun.* 10, 1983. <https://doi.org/10.1038/s41467-019-10003-8>
- Poole, P.H., 1995. Amorphous polymorphism. *Computational Materials Science* 4, 373-382. DOI: 10.1016/0927-0256(95)00044-9
- Powder Diffraction on the WEB, <http://pd.chem.ucl.ac.uk/pdnn/symm3/sgpfreq.htm>
- Rekis, T., 2020. Crystallization of chiral molecular compounds: what can be learned from the Cambridge Structural Database? *Acta Cryst.* B76, 307-315. <https://doi.org/10.1107/S2052520620003601>
- Ruby Dreamscape™ Cut, <https://www.johndyergems.com/gemstones/ruby-7397.html>
- Samotoin, N.D., 2011. Enantiomorphism of kaolinite: manifestation at the levels of elementary layer and microcrystals. *Crystallography Reports* 56, 327-334. DOI: 10.1134/S1063774511010202
- Shindo, H. et al, 2013. Asymmetric autocatalysis induced by cinnabar: Observation of the enantioselective adsorption of a 5-pyrimidyl alkanol on the crystal Surface. *Angew. Chem. Int. Ed.* 52, 9135 -9138. DOI: 10.1002/anie.201304284. See also the supporting information.
- Smith, P.P.K., 1979. The observation of enantiomorphous domains in a natural maghemite. *Contr. Mineral. and Petrol.* 69, 249-254. <https://doi.org/10.1007/BF00372327>
- Kenso Soai, K., et al, 1999. d- and l-Quartz-Promoted Highly Enantioselective Synthesis of a Chiral Organic Compound. *J. Am. Chem. Soc.* 121, 11235-11236. <https://doi.org/10.1021/ja993128t>
- Staples, L.W., 1935. Austinite, a new arsenate mineral, from Gold Hill, Utah. *American Mineralogist* 20, 112-119.
- Strunz, H., 1962. Fichtelit. Dimethyl-isopropyl-perhydropenanthren. *Naturwissen.*, 49, 9-10. doi:10.1007/bf00632826
- Symmetry@Otterbein, <https://symmotter.org/tutorial/intro>
- Támara, M., Preston, M.R., 2009. A statistical reassessment of the evidence for the racemic distribution of quartz enantiomorphs. *American Mineralogist* 94, 1556-1559. DOI: 10.2138/am.2009.3089
- Tanaka, Y., et al, 2008. Right handed or left handed? Forbidden X-ray diffraction reveals chirality. *Phys. Rev. Lett.* 100, 145502. DOI: 10.1103/PhysRevLett.100.145502
- Tanaka, Y., et al, 2010. Determination of structural chirality of berlinite and quartz using resonant x-ray diffraction with circularly polarized x-rays. *Phys. Rev. B* 81, 144104. DOI: 10.1103/PhysRevB.81.144104. Erratum: 2011. *Phys. Rev. B* 84, 219905(E). DOI: 10.1103/PhysRevB.84.219905
- The Mineral Cristobalite**, <https://www.minerals.net/mineral/cristobalite.aspx>
- The Mineral Quartz, <https://www.minerals.net/mineral/quartz.aspx>; %20https://www.mindat.org/min-3337.html
- The Quartz Page, <http://www.quartzpage.de/>
- The Quartz Page, [http://www.quartzpage.de/crs\\_forms.html](http://www.quartzpage.de/crs_forms.html)
- The Quartz Page, [http://www.quartzpage.de/gen\\_struct.html](http://www.quartzpage.de/gen_struct.html)
- The Structure of Materials, <http://som.web.cmu.edu/structures/S092-wollastonite.html>
- The Structure of Materials, <http://som.web.cmu.edu/structures/S097-alpha-quartz.html>
- Thomas, P.A. 1988. The crystal structure and absolute optical chirality of paratellurite,  $\alpha$ -TeO<sub>2</sub>. *J. Phys. C: Solid State Phys.* 21, 4611-4267. DOI 10.1088/0022-3719/21/25/009
- Thompson, A.L., Watkin, D.J., 2009. X-ray crystallography and chirality: understanding the limitations. *Tetrahedron: Asymmetry* 20, 712-717. doi:10.1016/j.tetasy.2009.02.025
- Tridymite, <https://en.wikipedia.org/wiki/Tridymite>
- Tuvi-Arad, I. et al, 2024. CSM software: Continuous symmetry and chirality measures for quantitative structural analysis. *J. Chem. Inf. Model.* in press. <https://doi.org/10.1021/acs.jcim.4c00609>
- Urusov, V.S., Nadezhina, T.N., 2009. Frequency distribution and selection of space groups in inorganic crystal chemistry. *Journal of Structural Chemistry* 50, 22-37. DOI:10.1007/s10947-009-0186-9
- Valentín-Pérez, Á. et al, 2022. Chirality determination in crystals. *Chirality* 34, 163-181. <https://doi.org/10.1002/chir.23377>
- Van Dyke, K.S., 1940. On the right- and left-handedness of quartz and its relation to elastic and other properties. *Proceedings of the Institute of Radio Engineers (I.R.E.)*, September, 1940, 399-406
- Van der Biest, O., Thomas, G., 1975. Identification of Enantiomorphism in Crystals by Electron Microscopy. *Acta Cryst.* A31, 70-76. <https://doi.org/10.1107/S0567739475000137>
- Vinegrad, E. et al, 2018. Circular Dichroism of Single Particles. *ACS Photonics* 5, 2151-2159. DOI: 10.1021/acsphotonics.8b00016
- Ward, R.M. et al, 2010. Enantiomorphic symmetry breaking in crystallization of molten sodium chlorate. *Chem. Commun.* 46, 7634-7636. DOI: 10.1039/c0cc02563a
- Watkin, D.J., and Richard Ian Cooper <R.I., 2020. Howard Flack and the Flack Parameter. *Chemistry* 2, 796-804. doi:10.3390/chemistry2040052
- Webmineral, <http://webmineral.com/crystal/Triclinic.shtml>

- Wenk, H.-R., 2006. Neutron Diffraction Texture Analysis. *Reviews in Mineralogy & Geochemistry* 63, 399-426. DOI: 10.2138/rmg.2006.63.15
- Williams, S.A., de Azevedo, J., 1967. Austinite from Gold Hill, Utah. *American Mineralogist* 52, 1224–1226.
- Wilson, P. 1979. Experimental investigation of etch pit formation on quartz sand grains. *Geological Magazine* 116, 477-482. DOI: 10.1017/S0016756800044472
- Winkelmann, A., Nolze, G., 2014. Chirality determination of quartz crystals using Electron Backscatter Diffraction. *Ultramicroscopy* 149, 58-63. <http://dx.doi.org/10.1016/j.ultramic.2014.11.013>
- Christopher J. Winta, C.J. et al, 2018. Second-harmonic phonon spectroscopy of  $\alpha$ -quartz. *Phys. Rev. B* 97, 094108. DOI: 10.1103/PhysRevB.97.094108
- Wukovitz, S.W., Yeates, T.O., 1995. Why protein crystals favour some space-groups over others. *Nat. Struct. Biol.* 2, 1062-7. doi: 10.1038/nsb1295-1062
- Yogev-Einot, D., Avnir, D., 2003. Quantitative symmetry and chirality of the molecular building blocks of quartz. *Chem. Mater.* 15, 464 – 472. <https://doi.org/10.1021/cm0207806>
- Yogev-Einot, D., Avnir, D., 2004. Pressure and temperature effects on the degree of symmetry and chirality of the molecular building blocks of low quartz, *Acta Cryst.* B60, 163–173. doi: 10.1107/S0108768104003647
- Yogev-Einot, D., Avnir, D., 2006. The temperature-dependent optical activity of quartz: from Le Chatelier to chirality measures. *Tetrahedron: Asymmetry* 17, 2723 – 2725. <https://doi.org/10.1016/j.tetasy.2006.10.004>
- Yogev-Einot, D., Avnir, D., 2007. Left/right handedness assignment to chiral tetrahedral AB<sub>4</sub> structures. *Tetrahedron: Asymmetry* 18, 2295–2299. <https://doi.org/10.1016/j.tetasy.2007.09.024>
- H. Zabrodsky, H., et al, 1992. Continuous Symmetry Measures, *J. Am. Chem. Soc.* 114, 7843-7851. <https://doi.org/10.1021/ja00046a033>
- H. Zabrodsky, H., Avnir, D., 1995. Continuous Symmetry Measures, IV: Chirality. *J. Am. Chem. Soc.* 117, 462-473. <https://doi.org/10.1021/ja00106a053>

**Disclaimer/Publisher's Note:** The statements, opinions and data contained in all publications are solely those of the individual author(s) and contributor(s) and not of MDPI and/or the editor(s). MDPI and/or the editor(s) disclaim responsibility for any injury to people or property resulting from any ideas, methods, instructions or products referred to in the content.